THESIS

Molecular Mechanism of Degradation of Chlorophyll in Higher Plants

Yasuyo Suzuki

Graduate School of Science and Engineering
Shizuoka University

June 2003

THESIS

Molecular Mechanism of Degradation of Chlorophyll in Higher Plants

高等植物におけるクロロフィル分解の分子機構

鈴木　康予

静　岡　大　学
大学院理工学研究科
環境科学専攻

2003 年 6 月

CONTENTS

Summary

Degradation of chlorophyll (Chl) in higher plants and algae was investigated throughout this study. This thesis consists of six Chapters including general introduction and five main subjects.

Changes of Chls and carotenoids from green and senescent cotyledons of radish (*Raphanus sativus*) were analyzed by high-performance liquid chromatography (HPLC) with photodiode array detection. Most Chl species degraded during senescence, while carotenoids showed different behavior in their metabolism depending on species. Carotenoids were classified roughly into three groups by their time-courses of concentration during senescence, i.e., increased, degraded and stabilizing groups (Chapter II).

The demethoxycarbonyl reaction of pheophorbide (Pheid) *a* in plants and algae was investigated. Two types of enzyme that catalyze alternative reactions in the formation of pyropheophorbide (PyroPheid) *a* were found. One enzyme, designated “pheophorbidase (Phedase)”, was purified nearly to homogeneity from the cotyledons of radish. This enzyme catalyzes the conversion of Pheid *a* to a precursor of PyroPheid *a*, C-13^2-carboxylpyro-pheophorbide *a*, by demethylation, and then the precursor is decarboxylated non-enzymatically to yield PyroPheid *a*. The other enzyme, termed “pheophorbide demethoxycarbonylase (PDC)”, was highly purified from the Chl *b*-less mutant NL-105 of *Chlamydomonas reinhardtii*. This enzyme had produced no intermediate as shown in the Phedase reaction, indicating that it converts Pheid *a* directly into PyroPheid *a*, probably by nucleophilic reaction. Phedase and PDC both consisted of senescence-induced and constitutive enzymes (Chapter III). Phedase showed three bands of 16.8, 15.9 and 11.8 kDa on sodium dodecyl sulfate (SDS)-polyacrylamide gel electrophoresis (PAGE). The partial N-terminal amino acid sequences for these bands of the purified Phedase (constitutive type) were determined. Based on their N-terminal amino acid sequences, partial cDNA of Phedase was cloned by a

combination of RT-PCR and RACE (Chapter IV).

To elucidate the late stage of Chl degradation, chemical oxidation products of Chl and porphyrin were analyzed by HPLC with detection of absorbance at 280 nm using a wide-pore, octadecyl polyvinyl alcohol polymer column and isocratic elution with acetonitrile-water (25%, v/v) containing 100 mM ammonium acetate. The determination of intermediary breakdown products of Chls in senescent leaves of higher plants was performed by HPLC technique that had been newly developed, as described above. In six plants including barley tested, degradation products were detected only in the senescent leaves of plants, except for radish, in which they were found both in pre- and senescent cotyledons. The degradation process and amounts of breakdown products of Chls depend largely on plant species and vary with length of senescence. The results clearly showed that Chls are degraded into low-molecular-weight hydrolytic compounds through monopyrroles (Chapter V).

The results of present studies on the Chl degradation in vitro are discuss in relation to the present understanding of Chl breakdown in intact plants, especially, some approaches toward the localization of breakdown of Chls. The author proposes the idea of the presence of extraplastidic and multiple degradation pathways in the breakdown of Chls (Chapter VI).

List of Abbreviations

BChl	bacteriochlorophyll
BPheid	bacteriopheophorbide
Chl	chlorophyll
Chlase	chlorophyllase
Chlid	chlorophyllide
DEAE	diethylaminoethyl
GC	gas chromatography
HA	hematinic acid
HEPES	N-[2-hydroxyethyl]piperazine-N'-[2-ethanesulfonic acid]
HPLC	high-performance liquid chromatography
k'	capacity factor
LC	liquid chromatography
MEM	methyl ethyl maleimide
MES	2-morpholinoethanesulfonic acid
MOPS	3-morpholinopropanesulfonic acid
MVM	methyl vinyl maleimide
ODP	octadecyl polyvinyl alcohol polymer
ODS	octadecyl silica
PAGE	polyacrylamide gel electrophoresis
PChl	protochlorophyll
PChlid	protochlorophyllide
PCR	polymerase chain reaction
PDC	pheophorbide demethoxycarbonylase
Phedase	pheophorbidase
Pheid	pheophorbide
Phe	pheophytin
PyroPheid	pyropheophorbide
RACE	rapid amplification of cDNA ends
R_f	rate of flow
RT-PCR	reverse transcriptase-PCR
SDS	sodium dodecyl sulfate
TLC	thin-layer chromatography
t_0	retention time of unretained solute
t_R	retention time
Tricin	N-[tris (hydroxymethyl) methyl]-glycine
Tris	tris (hydroxymethyl) aminomethane

Chapter I

General Introduction

The changes in color of leaves and ripening fruits are visible results of the breakdown of chlorophylls (Chls) as a consequence of senescence or maturation. As shown in Figure I-1, the pathway for the breakdown of Chl consists of several reaction steps. In the early stage of the degradation process, the modification of the side chains of the macro- and isocyclic rings of Chl occurs in reactions catalyzed by several enzymes (Brown et al. 1991; Shioi et al. 1991; Matile et al. 1996; Gossauer and Engel 1996). Subsequently, the tetrapyrrole macrocyclic ring is cleaved, probably by monooxygenase with the involvement of molecular oxygen (Curty et al. 1995; Hörtensteiner et al. 1998).

Information concerning enzymes involved in the modification of macro- and isocyclic rings has gradually accumulated in recent years. The first step in the degradation of Chl *a* is hydrolysis of the phytyl ester linkage catalyzed by chlorophyllase (EC 3.1.1.14), which forms chlorophyllide *a* and phytol (Tsuchiya et al. 1997; Takamiya et al. 2000 and references cited thererein). Next, a release of magnesium occurs from the macrocyclic ring and forms pheophorbide (Pheid) *a*. An activity catalyzing this reaction has been reported in algae and higher plants and has been considered to be due to an enzyme that had been designated "Mg-dechelatase" (Owens and Falkowski 1982; Ziegler et al. 1988; Shioi et al. 1991; Vicentini et al. 1995). Recently, Shioi et al. (1996a) found that this activity is not due to an enzyme, but to a low-molecular-mass, heat-stable substance, which they designated "Mg-dechelating substance". The highly purified substance is, however, specific not only for Mg^{2+}, but also for divalent cations. They therefore renamed it "metal-chelating substance".

The final step of macrocyclic ring modification is the conversion of formed Pheid *a* to pyropheophorbide (PyroPheid) *a*. Two types of enzyme that catalyze alternative reactions in the formation of PyroPheid *a* were found (Suzuki et al. 2002). One formation consists of two reactions: first, enzymatic conversion of Pheid *a* to a precursor of PyroPheid *a*, identified as C-13^2-carboxylpyropheophorbide *a*, and next, spontaneous conversion of the precursor to PyroPheid *a* (Shioi et al. 1996b, Watanabe et al. 1999). This

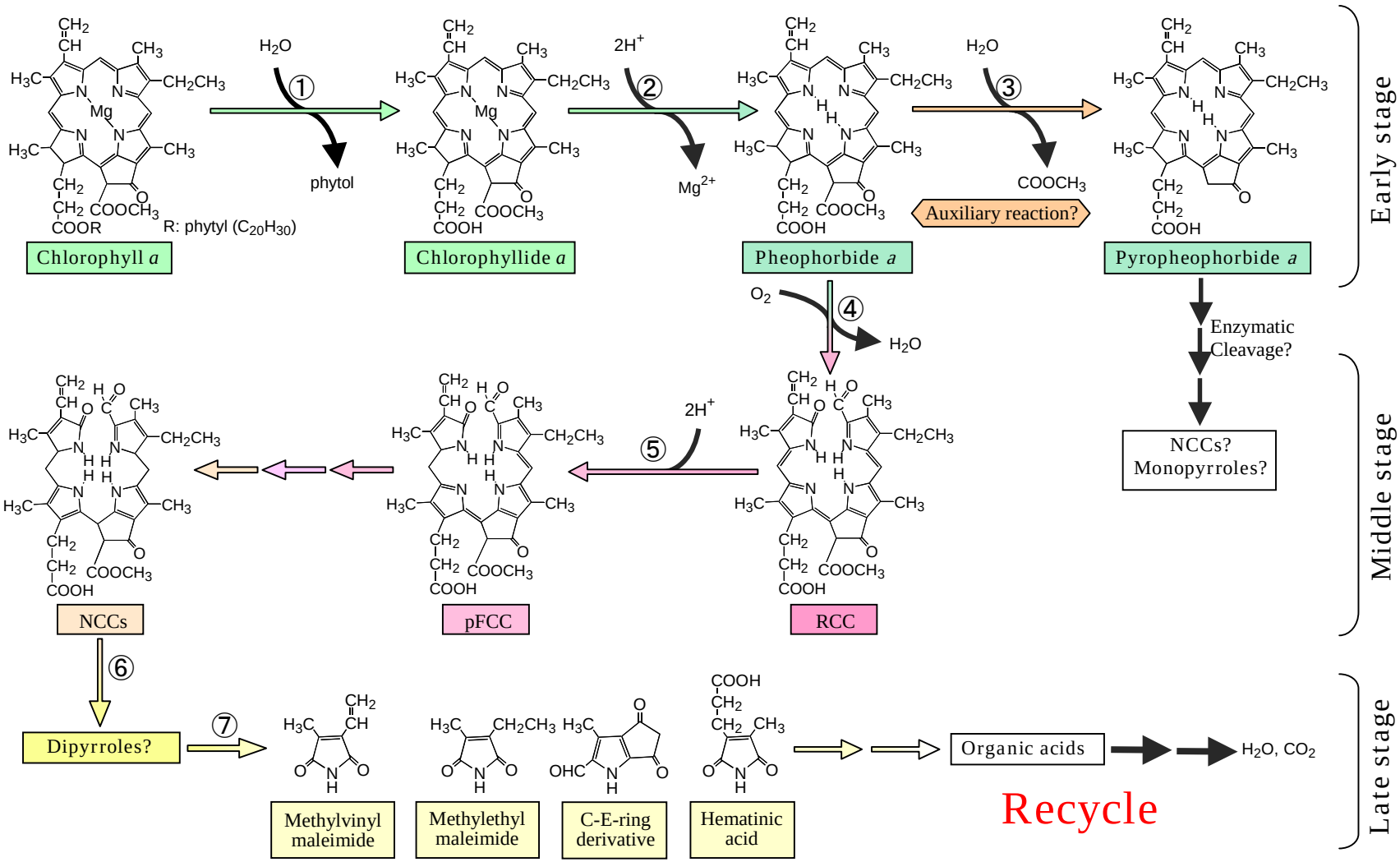

Fig. I-1. The tentative degradation pathway of Chl *a*. Steps 3 and 7 are main subjects of this study. The enzymes involved in each reaction step: ①, chlorophyllase; ②, metal-chelating substance; ③, Phedase / PDC; ④, monooxygenase; ⑤, red Chl catabolite reductase; ⑥⑦, enzymes (?).

Abbreviations: RCC, red Chl catabolite; pFCC, primary fluorescent Chl catabolite; NCCs, non-fluorescent Chl catabolites.

enzyme was designated "pheophorbidase (Phedase)" as a working name. This activity was detected in several but not all species of higher plants, and thus this reaction may be specific for certain plants. The other enzyme, termed “pheophorbide demethoxycarbonylase (PDC)”, was purified from the Chl *b*-less mutant NL-105 of *Chlamydomonas reinhardtii* (Doi, et al. 2001). This enzyme had produced no intermediate as shown in the Phedase reaction, indicating that it converts Pheid *a* directly into PyroPheid *a*, probably by nucleophilic reaction. Recently, we found that these enzymes consist of two types, senescence-induced and constitutive enzymes (Suzuki et al. 2002).

The subsequent reaction, oxidative cleavage of the tetrapyrrole macrocyclic ring is probably catalyzed by a monooxygenase, the so-called Pheid *a* oxygenase (Matile et al. 1996; Rodoni et al. 1997). The main catabolites of degraded Chls after this reaction were identified as derivatives of bilin (Kräutler et al. 1991; Engel et al. 1991; Mühlecker et al. 1993; Iturraspe and Moyano 1995; Doi et al. 1997). The accumulation of these derivatives has been reported in senescent leaves of several higher plants (Kräutler et al. 1991; Mühlecker et al. 1993; Iturraspe and Moyano 1995) and in culture medium of algae (Oshio and Hase 1969a, 1969b; Engel et al. 1991; Doi et al. 1997). It is unclear whether these bilin derivatives are further degraded and metabolized in the plants themselves or are transported into vacuoles (Hinder et al. 1996) and then exposed on ground when leaves fall. This is interesting issue with regard to plant nutrition.

The reactions involved in the breakdown of Chls or bilins into low molecular weight compounds are, however, poorly understood with the exception of the products of photodegradation of Chls. Previously, methyl ethyl maleimide has been found in the photo-bleached endproduct of Chl dissolved in solvents (Jen and Mackinney 1970). The formation of several hydrophilic colorless products, low molecular weight organic acids, was detected during photodegradation in Chl *a* adsorbed on lipophilic particles (Llewellyn et al. 1990a, 1990b). However, there is no evidence concerning the

formation of these degradation products of Chl in plant leaves.

To establish the intermediary degradation step of Chls, we developed a simple and rapid technique using HPLC to separate and identify the degradation products of Chls, especially monopyrrole derivatives (Suzuki et al. 1999). This chromatographic method, using a wide pore, ODP column, enables the separation of ethyl and vinyl species of maleimide, as well as hematinic acid and C-E-ring derivative of Chls, by a rather simple isocratic elution system with a buffered eluent. We successfully employed this technique to separate and analyze the degradation products of PyroPheid *a* by enzymatic oxidation with peroxidase, as a simple model of biological degradation (Suzuki et al. 1999), and detection of Chl breakdown products in the senescent leaves of higher plants (Suzuki and Shioi 1999).

In this thesis, we describe four main subjects on degradation of Chl in addition to General Introduction (Chapter I): Chapter II, Color changes in cotyledons of radish during senescence; Chapter III, Two enzymatic reaction pathways in the formation of PyroPheid *a*; Chapter IV, Purification and cloning of PyroPheid forming enzyme, Phedase, from radish; and Chapter V, HPLC analysis of products in the late stage of Chl degradation in the senescent leaves of radish and barley.

.

Chapter II

Color Changes in Cotyledons of *Raphanus sativus* during Senescence

Introduction

In the stages of leaf senescence or fruit ripening, the changes of color are observed. In this step, chlorophyll (Chl) and carotenoid catabolism are accompanied by the degradation of cellular organelles, especially chloroplasts. Pathway of Chl degradation consists of several reaction steps catalyzed by enzymes (Hörtensteiner 1999; Takamiya et al. 2000). Information concerning the Chl degradation and enzymes involved in the pathway has gradually accumulated in recent years as described in Chapter I.

Carotenoids play important roles in the assembly of light-harvesting complex as antenna pigments, and also protect the photosynthetic apparatus from photo-oxidative damage. Catabolism of carotenoids has been studied at fruits ripening (Bramley 2002) and flowers (Hirscberg 2001). In particular, tomato fruits have become a model system for other chromoplast-containing tissues, because prominent changes of color occur during ripening and abundant color mutants are utilizable (Bramley 2002). In contrast, little is known on formation and degradation of carotenoids in leaves. Generally a diminution of carotenoids is slower than that of Chls, which results in being unmasked carotenoids, although there are a few exceptions (Whitfield and Roean 1974; Biswal et al. 1983). In addition, xanthophyll esters occur in senescent leaf (Egger and Schwenker, 1966; Biswal et al., 1994; Biswal, 1995; Tevini and Steinmüller, 1985). During advanced stages of senescence, there is a significant increase in the amount of free fatty acids released from triacyl glycerols by the action of hydrolyzing lipases and free carotenoids released from thylakoids are esterified by these fatty acids, which are deposited in plastoglobuli (Tevini and Steinmüller 1985). As light-dependent metabolism of carotenoids, xanthophyll cycle is known. In the light, zeaxanthin is formed from violaxanthin via antheraxanthin by enzymatic de-epoxidation, and in the dark the reverse reaction occurs (Gross, 1991). This cycle is very important for protection of photosynthetic system at high light intensities, because of consuming excess absorbed energy (Bramley, 2002).

On the other hand, degradation of Chls and carotenoids are observed during dark-induced senescence. In the dark, because photolysis and photo-inhibition are suppressed, metabolisms of photosynthetic pigments assumed to be performed by enzymes. Thus, study on the dark-induce senescence is significant to exclude from the light effect.

Here, we quantitatively analyzed the pigments extracted from cotyledons of radish during dark-induced senescence by high-performance liquid chromatography (HPLC) with a photodiode array detector. Seven Chls and 14 carotenoids were detected and mostly identified. Three carotenoid groups which showed different behavior in their time-courses during senescence are discussed.

Materials and methods

Plant materials

Cotyledons of radish (*Raphanus sativus* L.) were purchased from a local market. Induction of senescence was carried out using excised cotyledons in distilled water and left in dark at 25°C according to the method described previously (Suzuki and Shioi 1999).

Pigment Extraction.

Pigments were extracted from cotyledons (0.2 - 0.4 g) that were removed from the seedlings at various periods of senescence by grinding with a 5 ml of cold (-20°C) 80% aqueous acetone. After filtration with a 0.45-μm syringe filter (Millipore, MA, USA), 10 μl of extracts were used for HPLC analyses.

HPLC analysis

HPLC was carried out with a model LC-10AT (Shimadzu, Kyoto) equipped with a column-temperature controller, using a Waters Symmetry C_8 column (150 x 4.6 mm)(Milford, MA, USA). Analysis of Chls and carotenoids was performed according to the method of Zapata et al. (2000). Pigments were

eluted at a flow rate of 1.0 ml per min at 25°C with a programmed binary gradient elution system according to the method. Solvents used were, A: methanol:acetonitrile:0.25 M aqueous pyridine solution (50:25:25, by volume), and B: methanol:acetonitrile:acetone (20:60:20, by volume). Separation was performed with a gradient containing six break points: 0 min (100:0, v/v), 22 min (60:40), 28 min (5:95), 38 min (5:95), 41 min (100:0), 42 min (100:0). Separated pigments were detected spectrophotometrically with a photodiode array detector (Shimadzu SPD-M10A), measuring from 340 to 740 nm and monitoring 4 channels at representative wavelengths of Chls and carotenoids, 410, 430, 440, and 450 nm.

Pigments and their quantifications

Chl *a*, Pheid *a,* PyroPheid *a* and β-carotene (Fig. II-1) were purchased from Wako Pure Chemical Industries (Osaka, Japan). Lutein, violaxanthin and zeaxanthin were obtained from DHI (Copenhagen, Denmark). Chl *b* was purified from spinach leaves (*Spinacia oleracea*) by sucrose-column chromatography according to the method of Perkins and Roberts (1962). Pheophytins (Phes) *a* and *b* were prepared by acidic treatment of the respective Chls (Perkins and Roberts 1962). Quantities of each pigment were calculated from standard curves. The standard curves were created for Chls and carotenoids from the relationships between concentrations and peak areas after HPLC. Identification and quantification of Chls such as Chlid *a*, Pheid *a* and PyroPheid *a* were carried out according to our previous method (Doi et al. 1997).

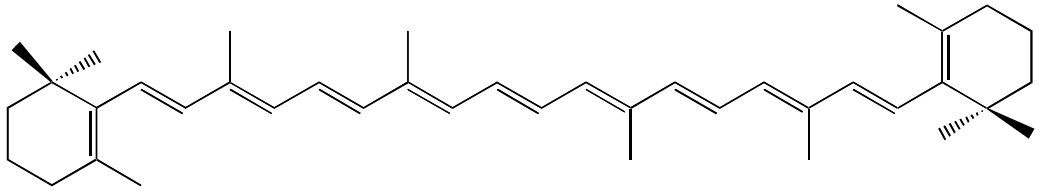

β-carotene

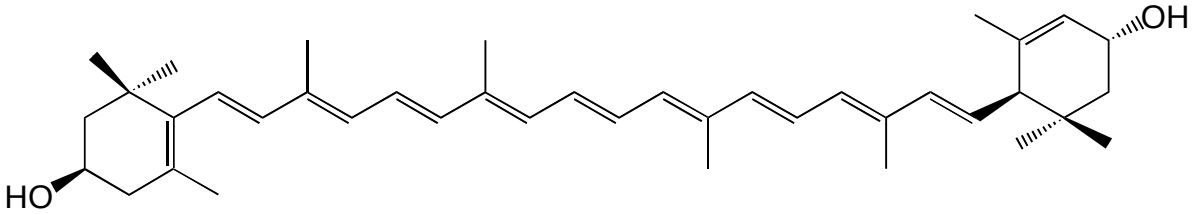

Lutein

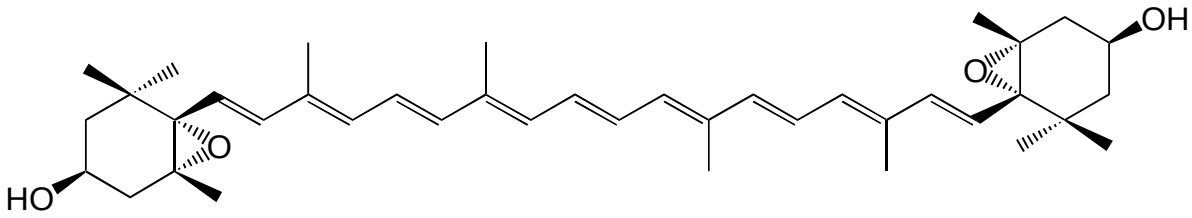

Violaxanthin

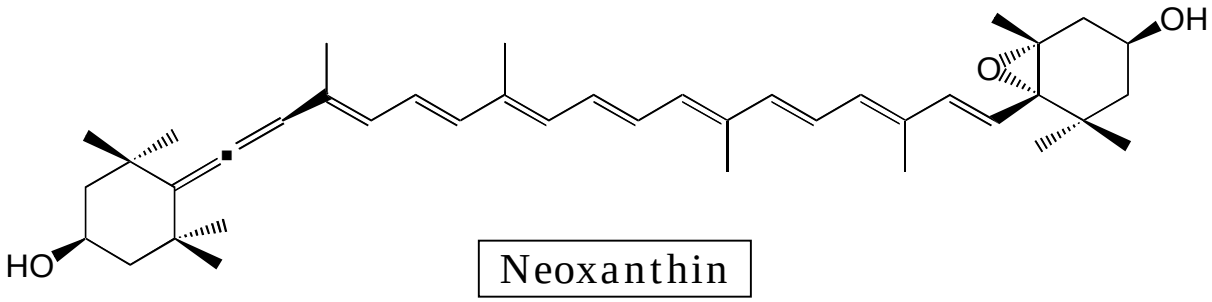

Neoxanthin

Fig. II-1. Structures of a carotene, β-carotene, and three xanthophylls, lutein, violaxanthin and neoxanthin.

Results

Peak identification

Acetone extracts from radish cotyledons were analyzed by HPLC using a photodiode array detector. Each peak was identified by comparison with HPLC retention times and absorption spectrum of the standards and also from the data of photodiode array detection. In this study, 21 peaks were detected (Table II-1 and Fig. II-2). Of these, 7 Chls (Chls *a* and *b* and their epimers, Chlids *a* and *b* and Phe *a*) and 5 carotenoids (neoxanthin, violaxanthin, zeaxanthin, lutein and β-carotene) (Fig. II-1) were identified from the comparison with peak spectral data and retention times of authentic samples after HPLC (Zapata et al. 2000).

Chlorophyll degradation during senescence

During senescence, the changes of Chl derivatives were analyzed (Figs. II-3 and II-4). Chls, Chlids and Phe *a* were detected, but not Pheids and PyroPheids (Fig. II-2 and Table II-1). Chls and Phe *a* contents in senescent cotyledons of radish were calculated from the results of HPLC analyses using the standard curves (Fig. II-3). The concentrations of Chls *a* and *b* estimated by HPLC were comparable to those measured by spectrophotometrical analysis according to the method of Mackinney (1941). When compared with Chls *a* and *b*, the quantity of Phe *a* and epimers of Chls *a* and *b* was low. Before senescence, the ratios of Chls were as follows: 0.013 for Phe *a* to Chl *a*; 0.014 for Chl *a´* to Chl *a*; and 0.003 for Chl *b´* to Chl *b*. Ratio of Chl *a* to Chl *b* tended to increase gradually during senescence. The Chl *a* to Chl *b* ratio was 3.5 in non-senescent leaves and reached about 4.0 after 3 days of senescence.

Figure II-4 shows the relative changes of each Chl derivative. Chlids *a* and *b* showed the highest rate of degradation among Chl derivatives; at 4-day-senecsence, approximately 80% of Chlid *a* and Chlid *b* completely disappeared. Contrary to Chlid species, Phe *a* was degraded slowly. Chl *b* seemed to be degraded faster than Chl *a*. This was the case in Chlid species.

Table II-1. Identification of chlorophylls and carotenoids by HPLC in green and senescent cotyledons of *Raphanus sativus*.

Marks	t_R (min)	Identification	λ_{max} (nm)		
1	5.7	Chlorophyllide *b*	464		651
2	11.7	Chlorophyllide *a*	428		663
3	20.2		417	441	469
4	22.3	Neoxanthin	414	437	464
5	24.1	Violaxanthin	417	436	469
6	28.7		414	436	464
7	29.1			442	463
8	30.4	Zeaxanthin		436	458
9	30.7	Lutein		446	474
10	31.7			443	470
11	32.0			441	468
12	34.9	Chl *b*	462	599	647
13	35.2	Chl *b* epimer	459		641
14	36.6	Chl *a*	431	661	662
15	37.0	Chl *a* epimer	432		663
16	37.6			447	473
17	38.8	Pheophytin *a*	408	606	665
18	39.1			448	473
19	39.7	β-carotene		452	475
20	40.5			441	469
21	31.0		422	447	469

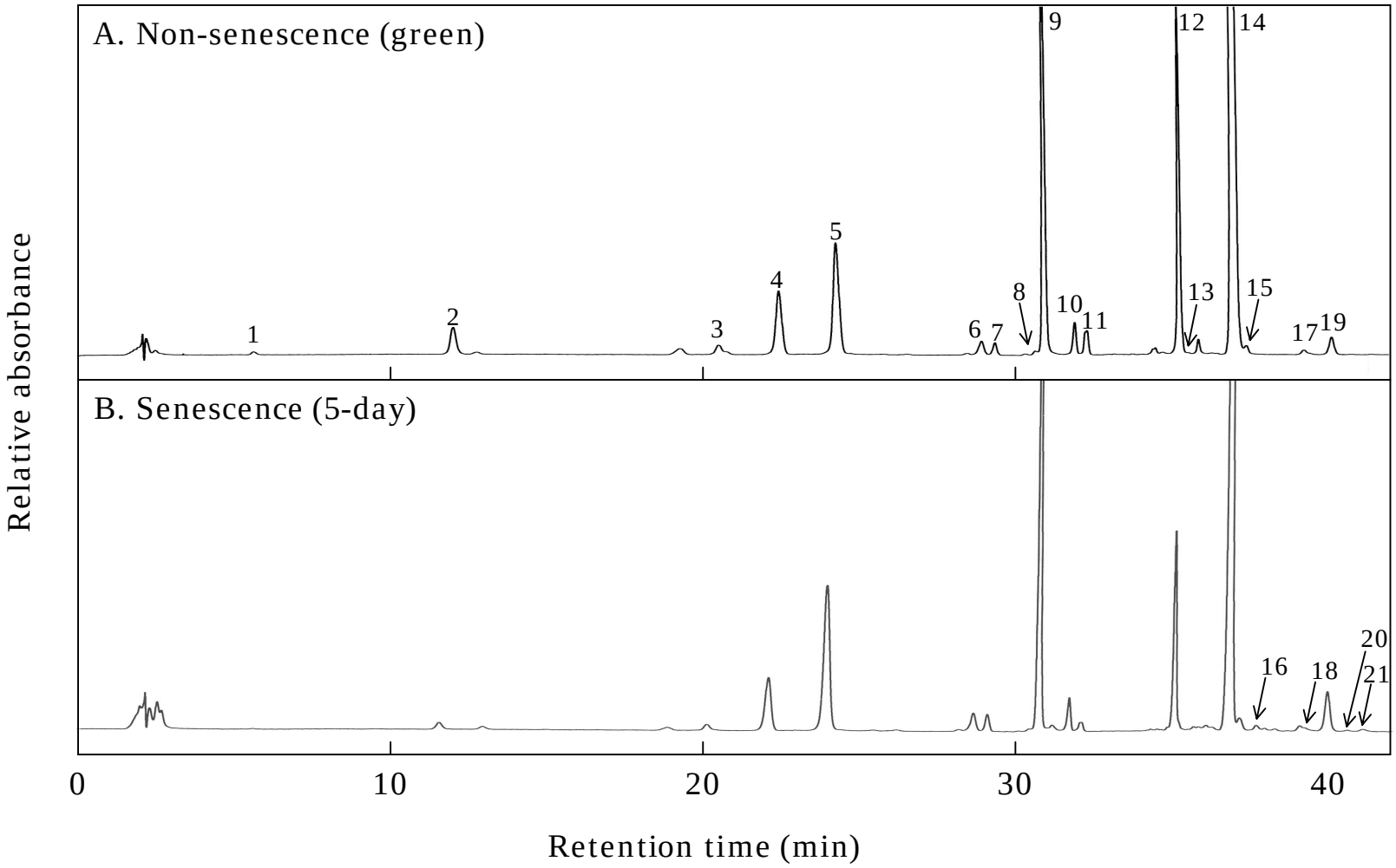

Fig. II-2. HPLC elution profiles of Chls and carotenoids from 80% aqueous acetone extracts of non-senescent (A) and senescence (B) cotyledons of *Raphanus sativus*. Detection was carried out at 430 nm. Chromatographic conditions are described in the text.

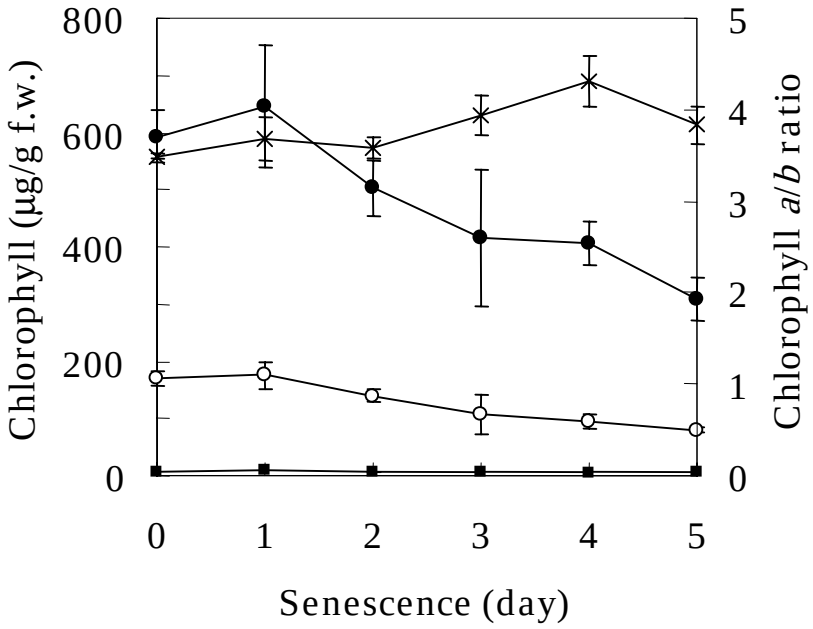

Fig. II-3. Changes of concentration of Chls and Chl *a* to Chl *b* ratio in extract of radish cotyledons during senescence. The concentrations were calculated from the standard curves created by peak areas of HPLC analyses. ●, Chl *a*; ○, Chl *b*; ■, Chl *a´* (Chl *b´* and Phe *a* are not plotted, but are equivalent to Chl *a´*) ; ×, ratio of Chl *a* to Chl *b*. All values are the mean ± SD (n = 3).

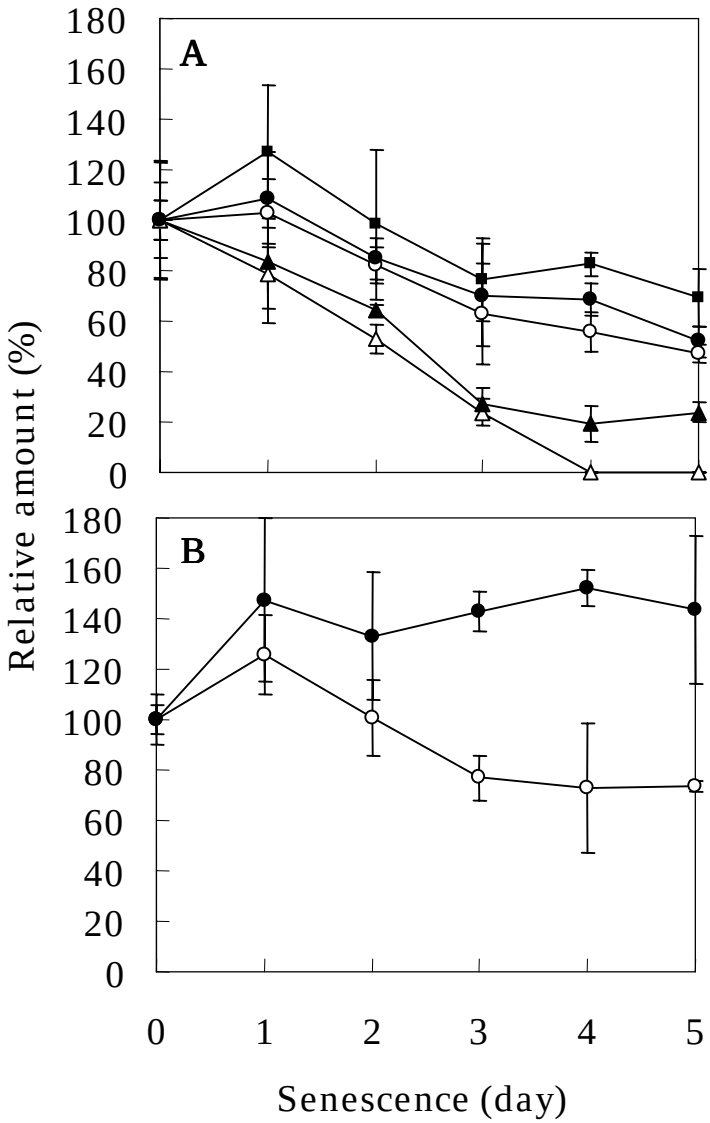

Fig. II-4. Relative changes in Chls during senescence. The values of peak area measured by HPLC are expressed relative to non-senescence as control (100%). (A) Chl derivatives, (B) Chls *a* and *b* epimers. ●, Chl *a*; ○, Chl *b*; ▲, Chlid *a*; △, Chlid *b*; ■, Phe *a*. All values are the mean ± SD (n=3).

These results suggest that Chl *a* species might be more stable than Chl *b* species. Epimer of Chl *b* decreased similarly to Phe *a*, whereas Chl *a* epimers increased (Fig. II-4B). Formation of epimers of Chls *a* and *b* is known to occur by heating such as microwave cooking (Chen and Chen 1993) and processing of tea (Suzuki and Shioi, in press). Another possibility is production of epimers during extraction. Concentrations of Chls and their epimers increased largely in the extracts after storage for 1 h at room temperature (data not shown). Epimer of Chl *b* was more labile than that of Chl *a* as well as Chl *b* and their derivatives.

Carotenoid changes during senescence

In radish leaves, 14 species of carotenoids including β-carotene and lutein were detected using HPLC system. These carotenoids were divided into three groups by their time-courses during senescence. First group is that concentration of carotenoids decreased accompanying senescent progress like Chls (Fig. II-5A). Four carotenoids containing neoxanthin and zeaxanthin degraded during senescence. Neoxanthin drew a similar decreasing curve to Phe *a* (Fig. II-4A); it increased to about 120% at one day of senescence and then decreased. Zeaxanthin was stable until two days and turned to metabolize at three days. In addition, unidentified two carotenoids decreased to about 75% in 1-day-senescent leaves.

Second group is the carotenoids that showed almost no change in concentration even after 5-day-senescent leaves (Fig. II-5B). This group was comprised of five carotenoids. Violaxanthin and lutein did not fluctuate. Due to no change of violaxanthin and decrease of zeaxanthin, xanthophyll cycle is considered to not function in both forward and reverse reactions under this condition. Interestingly, the other three carotenoids, all unknown, returned to the same level after slightly increased, however these carotenoids differed time of reaching maximum, for example, peak 10 (t_R = 31.2) reached at 1 to 2 day, peak 7 (t_R = 29.5) at 2 to 3 day and peak 6 (t_R = 28.5) at 4 day.

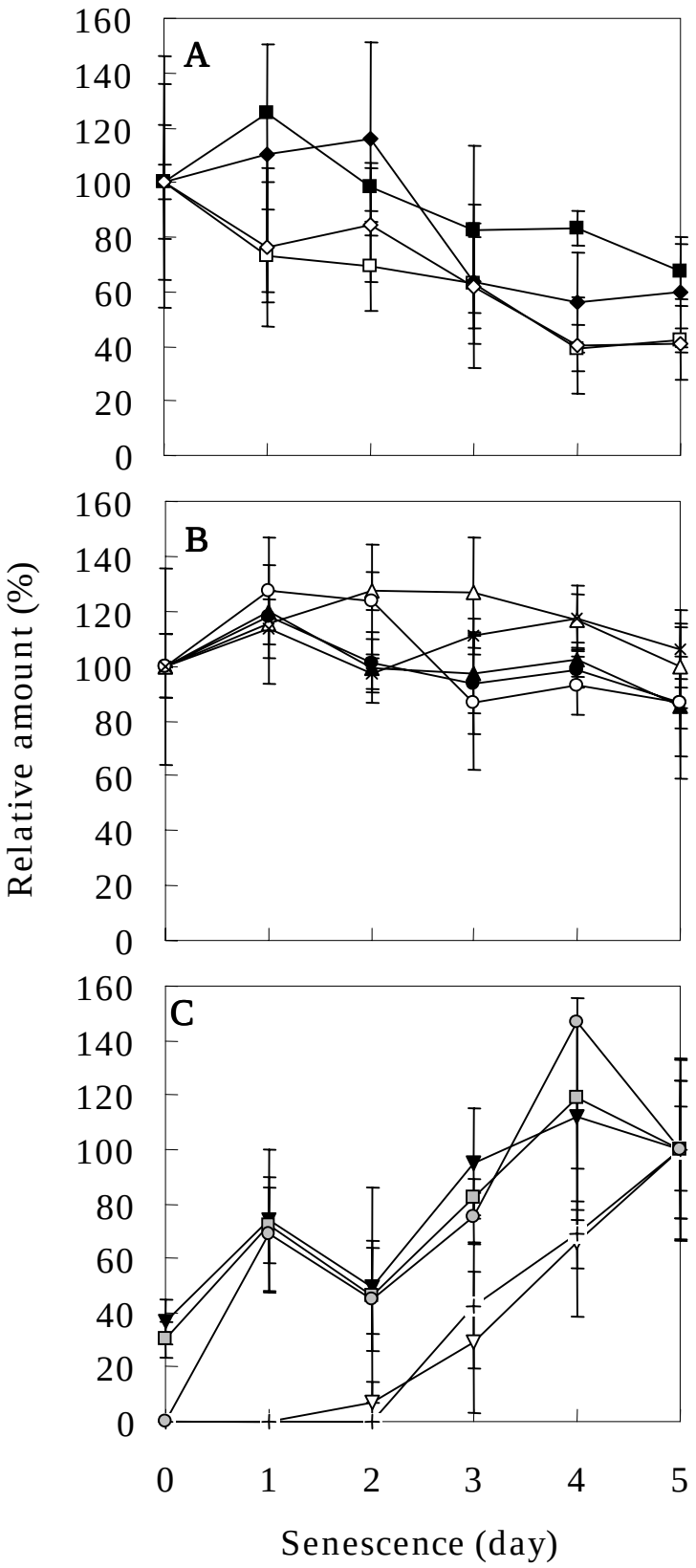

Fig. II-5. Relative changes in carotenoids during senescence. The values of peak area by HPLC are expressed relative to non-senescence as control. (A) “degraded” group; (B) “stabilizing” group; (C) “increaseing” group. ■, neoxanthin; ◆, zeaxanthin; □, peak 3; ◇, peak 11; ▲, violaxanthin; ●, lutein; ×, peak 6; △, peak 7; ○, peak 10; ▼, β-carotene; ▽, peak 16; ▢, peak 18; ◍, peak 20; +, peak 21. Peak number of unknown carotenoids corresponds to those of Table II-1 and Fig. II-1. All values are the mean ± SD (n = 3).

Carotenoids that increased in concentrations during senescence belonged to the third group (Fig. II-5C). There were five carotenoids in this group. Two carotenoids (peak 18 and β-carotene) existed constitutively and were increased by formation during senescence. Other three carotenoids were not detected before senescence, but emerged during senescence as small peaks by HPLC analysis. Unknown three carotenoids were strongly retained in column, indicating that they have strong hydrophobic property. From the appearance during senescence and the strong hydrophobicity, they were presumed to be esterified carotenoids (Biswal 1995).

Discussion

This article presents the changes of color pigments, Chls and carotenoids, during dark-induced senescence in cotyledons of *R. sativus.* To minimize the generation of free radicals by light, here being used the dark condition for the induction of senescence, the pigment changes might be caused by enzyme reactions (Biswal 1995). Chls, except for epimer of Chl *a*, were degraded during senescence. On the other hand, carotenoids were classified roughly into three types by their time-courses of concentration during senescence, for instance, increased, degraded, and stabilizing groups. This further suggests that with different from Chl degradation during senescence, metabolism of carotenoids were not only deteriorative, but also generative in part depending on species.

The Chl derivatives, Pheid and PyroPheid, could not detected in cotyledons of radish. This indicates that the turnover of Pheid species in radish cotyledons might be so fast that Pheid cannot accumulate. We previously reported that in radish cotyledons, the appearance of monopyrrole derivatives, such as hematinic acid and methyl ethyl maleimide, was earlier than in barley leaves (Suzuki and Shioi 1999).

On the degradation of free Chls and carotenoids, Tevini and Steinmüler (1985) reported that released carotenoids were turned into carotenoid esters by

a combination of free fatty acids and deposited in plastoglobuli. In this study, increase in unknown carotenoids was observed during senescence and was supposed to be carotenoid esters. If this is the case, it is presumed that carotenoid esters formed in senescent leaves of radish would be metabolized after deposited in plastoglobuli.

Carotenoids play an important role in the assembly of light-harvesting complex as accessory light-harvesting pigments. The composition of carotenoids is dependent on plant species (Gross 1991) and environmental factors (Biswal 1995, references cited therein). In radish cotyledons, β-carotene, lutein and violaxanthin were stable and neoxanthin declined during senescence. Among four main carotenoids, β-carotene is connected with reaction centers of photosystem and xanthophylls (lutein, violaxanthin and neoxanthin) with light-harvesting complex. It is reported that light-harvesting complex II and D1 protein were degraded by dark-induced senescence in soybean leaves (Guiamét et al. 2002). As shown here, most carotenoids were, however, stable, despite plastid proteins decreased during senescence. It is puzzling whether these carotenoids were also accumulated in plastoglobuli or stayed with another way. Through the movement of photosynthetic pigments, a clue that where and how chloroplasts and their pigments undergo the degradation may be found.

The ratio of Chl *a* to Chl *b* exhibited a gradual increase during senescence. Ito et al. (1993) reported that Chl *b* was converted to Chl *a*. Perhaps, Chl *b* conversion will contribute to raise the value of Chl *a/b.* Increase in Chl *a/b* ratio means that Chl *a* is more stable than Chl *b*. Considering the stability of β-carotene as well as Chl *a*, it is possible that reaction center of photosystem is presumed to be slowly degraded than antenna proteins.

In conclusion, Chl species degraded during senescence, while carotenoids had complex behavior in their time-courses depending on species.

Chapter III

Two Enzymatic Reaction Pathways in the Formation of Pyropheophorbide *a*

Introduction

The accumulation of pheophorbide (Pheid) *a* derivatives has been reported in the breakdown of chlorophylls (Chls) in a variety of photosynthetic organisms such as higher plants, algae, and bacterial cells. For instance, tobacco cells (Schoch and Vielwerth 1983), *Citrus unshiu* fruits (Shimokawa et al. 1990), *Chenopodium album* (Shioi et al. 1991), rape cotyledons (Langmeier et al. 1993), *Skeltonema* sp. extracts (Owens and Falkowski 1982), *Chlorella fuska* cells (Ziegler et al. 1988), *Euglena* sp. cells (Schoch et al. 1981), and *Rhodobacter sphaeroides* cells (Haidl et al. 1985). The occurrence of Pheid derivatives in such diverse species indicates that their formation might be a general step in Chl breakdown. Previously, we demonstrated the presence of an enzyme involved in the conversion of Pheid *a* to pyropheophorbide (PyroPheid) *a* in extracts of leaves from *Ch. album* (Shioi et al. 1996b) and characterized the enzyme (Watanabe et al. 1999). The enzyme called pheophorbidase (Phedase) catalyzes the conversion of Pheid *a* to a precursor, C-13^2-carboxylpyropheophorbide *a*, followed by the spontaneous decarboxylation of the precursor to PyroPheid *a*. This enzyme is, however, distributed in limited plant species (cf. Table III-3).

During the study of Chl degradation, we found an enzymatic activity that catalyzes PyroPheid *a* formation in mutant cells of *Chlamydomonas reinhardtii* (Doi et al. 2001). Close inspection of reaction products using a partially purified enzyme showed that no intermediate appeared before the PyroPheid *a* formation. It seems that an intermediate is not involved in the enzymatic reaction, and thus the enzyme catalyzes a direct release of the methoxycarbonyl moiety from Pheid. We therefore distinguished this enzyme from the former Phedase and designated it pheophorbide demethoxycarbonylase (PDC). Formation of PyroPheid *a* from Pheid *a* catalyzed by Phedase and PDC is illustrated in Figure III-1.

In order to understand the mode of reaction of these enzymes, we have purified the enzymes and compared their various properties, including the

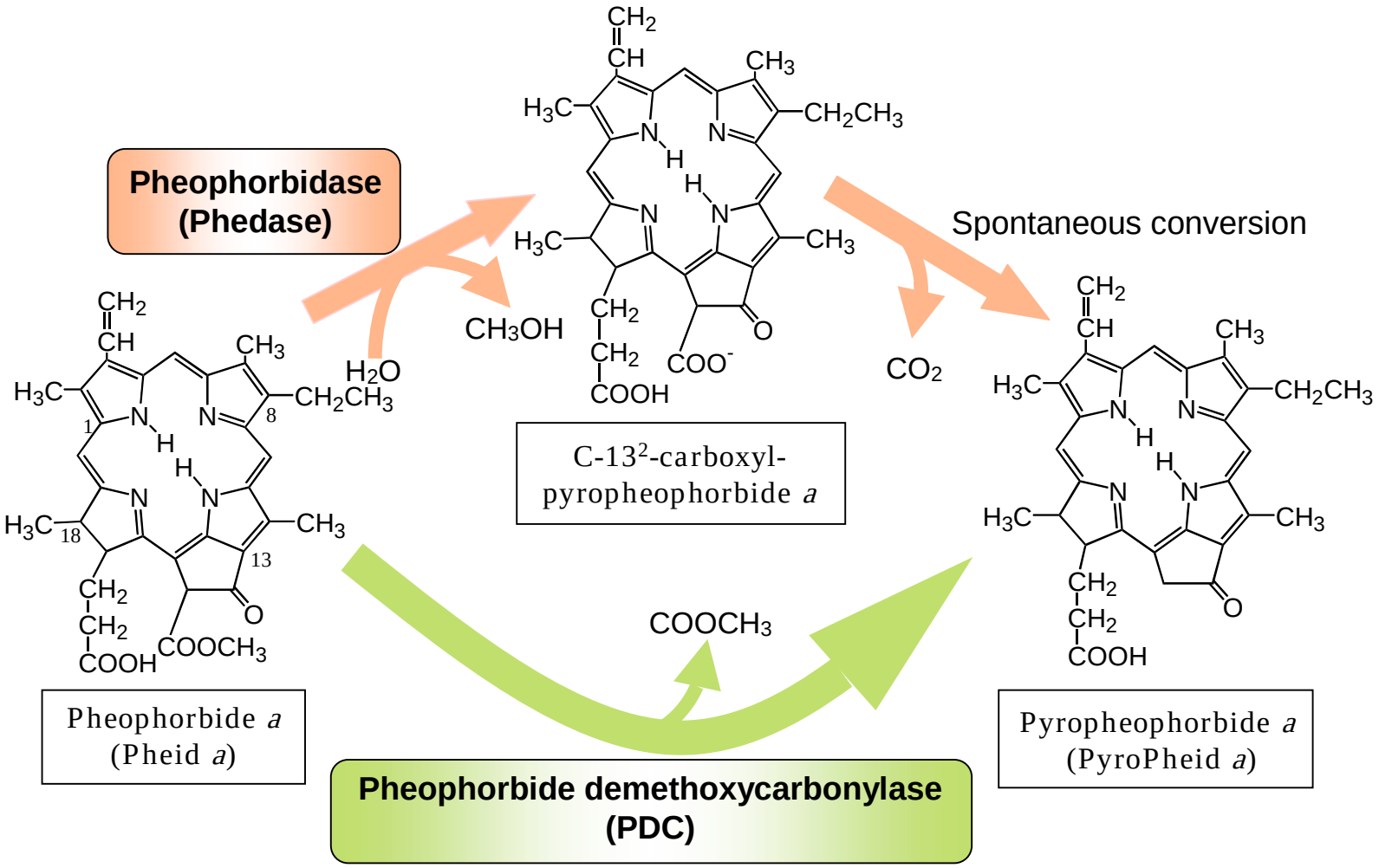

Fig. III-1. Demethoxycarbonyl reaction of pheophorbide *a*. Two enzymatic reactions are considered. One reaction, catalyzed by pheophorbidase (Phedase), is composed of two steps: conversion of pheophorbide *a* to a precursor, C-13^2-carboxylpyropheophorbide *a*, followed by spontaneous conversion of the precursor to pyropheophorbide *a*. The other reaction catalyzed by pheophorbide demethoxycarbonylase (PDC) is considered to be a direct conversion of pheophorbide *a* to pyropheophorbide *a* by nucleophilic reaction.

effect of inhibitors. Our results showed that the effect of the reaction product, methanol, on the activity of these enzymes differed between Phedase and PDC. In this report, we summarize the properties of these enzymes, Phedase purified from radish and PDC from *C. reinhardtii*, and propose the existence of two alternative pathways in the demethoxycarbonyl reaction of Pheid.

Materials and Methods

Plant materials

Cotyledons of radish (*Raphanus sativus* L.) were purchased from a local market. Induction of senescence was performed according to the method described previously (Suzuki and Shioi 1999). Wild and Chl *b*-less mutant NL-105 of *Chlamydomonas reinhardtii* were used. The algal cells were grown for 4 days in the light, followed by 3 days in the dark as described previously (Doi et al. 1997).

Chlorophylls

Chl *a*, Pheid *a* and PyroPheid *a* were purchased from Wako Pure Chemical Industries (Osaka, Japan). Chlorophyllide (Chlid) *a* was prepared from Chl *a* by enzymatic reaction using a chlorophyllase (EC 3.1.1.14.) prepared from *Ch. album* (Tsuchiya et al. 1997). The concentrations of Pheid *a* and PyroPheid *a* were determined spectrophotometrically as described previously (Doi et al. 1997).

Enzyme assay

The activity of the enzymes was assayed basically according to the methods described by Shioi et al. (1996b) for Phedase and by Doi et al. (2001) for PDC. For assay of Phedase activity, the reaction mixture consisted of 20 mM sodium potassium phosphate buffer (pH 7.0), 160 μM Pheid *a* (in final 20% (v/v) acetone) and Phedase preparation in a total volume of 100 μl. After

incubation in darkness at 30°C for 10 min, the reaction was terminated by adding 200 µl acetone. The amount of C-13^2-carboxylpyropheophorbide *a* formed was assayed using the HPLC system described below.

PDC activity was determined in a reaction mixture containing 20 mM MOPS-NaOH (pH 7.2), 40 µM Pheid *a* (in 0.1% Triton X-100) and enzyme solution in a total volume of 40 µl. The reaction was carried out in darkness at 37°C for 90 min and stopped by the addition of 160 µl acetone. Formation of PyroPheid *a* was quantified by HPLC as PDC activity.

HPLC analysis of the pigments was carried out according to our previous method with a slight modification (Shioi et al. 1996b). Briefly, HPLC was performed using a Zorbax ODS column (250 x 4.6 mm) (Agilent Technologies, Inc., CA, USA). Pigments were eluted isocratically with methanol-2 M ammonium acetate (95/5, v/v) at a flow rate of 1.0 ml per min at room temperature (ca. 25°C). The pigments were monitored spectrophotometrically at 410 nm and quantified by an integrator. Peak areas were used for the calculation of the enzyme activity.

Purification of Phedase

Senescent cotyledons of radish (ca. 3,900 g) were homogenized with 20 mM sodium potassium phosphate buffer (pH 7.0) at 4°C in a blender. The homogenate was filtered through six layers of cotton gauze and centrifuged at 17,000 x g for 30 min at 4°C. The cell-free extract was incubated at 60°C for 10 min and centrifuged 12,000 x g for 15 min. The supernatant was fractionated with 30% to 70% saturation of ammonium sulfate. The precipitate was dissolved with a small volume of 20 mM Tris-HCl (pH 7.5) and dialyzed against the same buffer. The enzyme solution was applied to a column of DEAE-Toyopearl (2.5 x 8 cm) previously equilibrated with 20 mM Tris-HCl (pH 7.5) and eluted with the same buffer containing a linear gradient of NaCl (0-0.35 M). Fractions eluted about 0.1-0.14M NaCl as senescence-induced (type 1) and 0.15-0.2 M as constitutive (type 2) were pooled. The

following purification procedures were carried out separately. After adding ammonium sulfate to 25% saturation, the enzyme solution was applied to a Butyl-Toyopearl column (2.5 x 8 cm) previously equilibrated with 20 mM Tris-HCl (pH 7.5) containing 25% saturation of ammonium sulfate and eluted with the same buffer containing a reverse-linear gradient of ammonium sulfate (25-0% saturation). Fractions eluted about 0-6% saturation for type 1 and 6-12% saturation for type 2 were pooled. The active fraction was dialyzed against 5 mM sodium potassium phosphate buffer (pH 7.0) and charged onto a column of hydroxyapatite (2.5 x 1 cm) which had been equilibrated with the same buffer. The column was eluted with 0.1 M sodium potassium phosphate buffer (pH 7.0). The pooled enzyme solution was applied to a column of Toyopearl HW-55 (2.5 x 90 cm) equilibrated with 20 mM Tris-HCl (pH 7.5) containing 0.15 M NaCl. Active fractions were collected and again applied to a Butyl-Toyopearl column in a similar manner as described above.

Purification of PDC

Algal cells (40 g) were suspended in 5 volumes of 20 mM MOPS buffer (pH 7.2). The cells were disrupted by ultrasonication for 5 min. Unbroken cells and large debris were removed by centrifugation at 20,000 x g for 30 min. The supernatant was further centrifuged to clarify it at 140,000 x g for 2 h. After ammonium sulfate was added to the resulting clear, yellowish supernatant to 1 M, the solution was loaded onto a Phenyl-Toyopearl column (1.6 x 5 cm) (Tosoh, Tokyo) previously equilibrated with the 20 mM MOPS buffer (pH 7.2) containing 1 M ammonium sulfate. The protein was eluted with a reverse-linear gradient from 1 to 0 M ammonium sulfate in 20 mM MOPS buffer (pH 7.2). The active fractions that were eluted around a concentration of 0.2 M ammonium sulfate were pooled and dialyzed against to 20 mM MOPS buffer (pH 7.2). The dialyzed fraction was applied to a DEAE-Toyopearl column (2.2 x 10 cm) (Tosoh, Tokyo) equilibrated with the same buffer. Unbound protein was washed with 20 mM Tricine buffer (pH 8.5),

and the bound protein was eluted with a linear gradient of 0 to 0.4 M NaCl in the same buffer. Fractions (2 ml) were collected and assayed for enzyme activity. The fractions eluted around 0.15-0.2 M NaCl were pooled and concentrated by Centriflo (Amicon, MA, USA). The concentrated protein was charged onto a column (2.2 x 60 cm) of Sephacryl S-300 Fine (Pharmacia, UK) equilibrated with 20 mM MOPS buffer containing 0.15 M NaCl. The protein was eluted with the same buffer at a flow rate of 30 ml/h. Fractions (2 ml) were collected and assayed for the activity. Active fractions were pooled, dialyzed against 10 mM MOPS buffer (pH 7.2) and concentrated by Centriflo.

Protein determination

Protein concentrations were determined using a BCA Protein Assay Kit (Pierce, IL, USA) with bovine serum albumin as a standard.

Results

Purification of enzymes

Most of the activities of both Phedase and PDC were retained in the supernatant fractions after ultracentrifugation of cell-free extracts, indicating that these enzymes are soluble proteins. Purification of these proteins was performed further through several chromatography steps, for example, ion-exchange, hydrophobic, and gel filtration. Phedase enzyme activity was separated into two peaks in the chromatography of DEAE- and Butyl-Toyopearl. Phedases separated by DEAE-Toyopearl were termed type 1 and type 2, according to their order of elution. In the chromatography of Butyl-Toyopearl, type 2 was eluted prior to type 1, indicating that elution order of these enzymes was reversed in hydrophobic separation. Type 1 appeared only after senescence and type 2 was almost no change after senescence. Thus, senescence-induced (type 1) and constitutive (type 2) were distinguished chromatographically. This indicates that type 1 is not the same protein

produced by up regulation, but isozyme induced by senescence. We purified these two types of Phedase from radish nearly to homogeneity. PDC also consisted of senescence-induced and constitutive enzymes, but only the senescence-induced type of PDC was obtained from a mutant of *C. reinhardtii*, because quantities of constitutive PDC were too small to purify. A similar PDC activity was also observed in wild type cells of *C. reinhardtii*. In this study, however, we have purified from the mutant cells used in the previous study (Doi et al. 2001). Phedases from cotyledons of radish were separated by DEAE-Toyopearl and purified 3,397- and 3,017-fold for senescence-induced (type 1) and constitutive types (type 2), respectively. PDC (senescence-induced type) was purified more than 80-fold from the crude extracts of mutant cells of *C. reinhardtii* basically according to the method described previously (Doi et al. 2001).

Molecular and enzymatic properties of Phedase and PDC

Some properties of Phedase and PDC are compared in Table III-1. Only the senescence-induced type of PDC from *C. reinhardtii* is presented due to the difficulty of purification of the constitutive type, as described above. The purified Phedase type 1 migrated as a single band with the respective molecular mass of 57 kDa on SDS-PAGE. The molecular weight of Phedase type 1 determined by gel filtration using Toyopearl HW-55 was 113,000. In addition, a mixture of Phedase types 1 and 2 emerged at the same peak on gel-filtration chromatography, indicating that these enzymes have the same molecular weight of 113,000, probably with a homotetramer (for details, see Chapter IV). PDC appeared as one major band with a molecular mass of 87 kDa and several faint bands on SDS-PAGE. The native molecular weight of PDC was determined to be 170,000 by Sephacryl S-300 gel filtration. These results suggest that PDC consisted of a homodimer. The native molecular mass of Phedase is similar to that of *Chenopodium* Phedase (Watanabe et al. 1995), although the *Chenopodium* enzyme had heterosubunit structure.

Table III-1. Properties of Phedase and PDC

Property	Phedase		PDC	
	type 1	type 2		
Enzyme type	Senescence-induced	Constitutive	Senescence-induced	Constitutive
Molecular weight	113,000	113,000	170,000	Trace
Subunit	Tetramer	Tetramer	Dimer	
*K*m (Pheophorbide *a*)	14 μM	15 μM	283 μM	
pH optimum	pH 7.0-7.5	pH 6.5	pH 7.2	
Activation energy	15.9 kcal	12.3 kcal	8.5 kcal	
Thermostability (50% lost)	67.5℃	67.5℃	56.0℃	

Since these enzymes showed Michaelis-Menten kinetics, the K_m values for Pheid *a* of Phedase and PDC were determined from a Lineweaver-Burk plot. The calculated K_m values of Phedases were 14.1 μM and 15.1 μM for types 1 and 2, respectively, and 283 μM for PDC. Thus, radish Phedases had about 20-fold higher affinity for Pheid *a* than PDC did. Substrate specificity for other Chl species was also tested on these two enzymes. These enzymes were highly specific for Pheid *a* and did not show any activity for Chls, Chlids and pheophytins (Phes). To determine the effect of pH on the enzymatic activity, 60 mM MES-HEPES-Tricine buffer was used for an incubation medium in the pH range from 5.5 to 9.0. Both senescence-induced enzymes, type 1 Phedase and PDC, had very similar pH optima of 7.2 and 7.0-7.5, respectively, whereas type 2 of Phedase, the constitutive enzyme, showed a slightly different pH optimum at pH 6.5. Activation energy was calculated from a slope of Arrhenius plots at the temperature range from 20 to 60°C. There was a 7 kcal difference in activation energy between the senescence-induced types of Phedase (type 1) and PDC; however, they were considered to be within the same range. The heat stability of the enzyme activities was in the temperature range of 30°C to 80°C. Both Phedases and PDC showed almost identical heat stability and lost 50% of their activities at 56°C for PDC and 67.5°C for Phedase types 1 and 2.

Effect of inhibitors on the enzyme activities

We reported that methanol is produced as a product in the Phedase reaction, and inhibits Phedase activity (Shioi et al. 1996b). If PDC had the same reaction mechanism as Phedase, its enzyme activity might also be inhibited by methanol. Therefore, the effects of methanol and reaction-product analogues on these enzymes were tested. As shown in Fig. III-2, both Phedases, types 1 and 2, were inhibited by methanol very similarly to 20% at 1 M (4.0%, v/v), but not by ethanol, whereas PDC was inhibited equally by both methanol and ethanol. PDC seems to be more susceptible to organic solvents

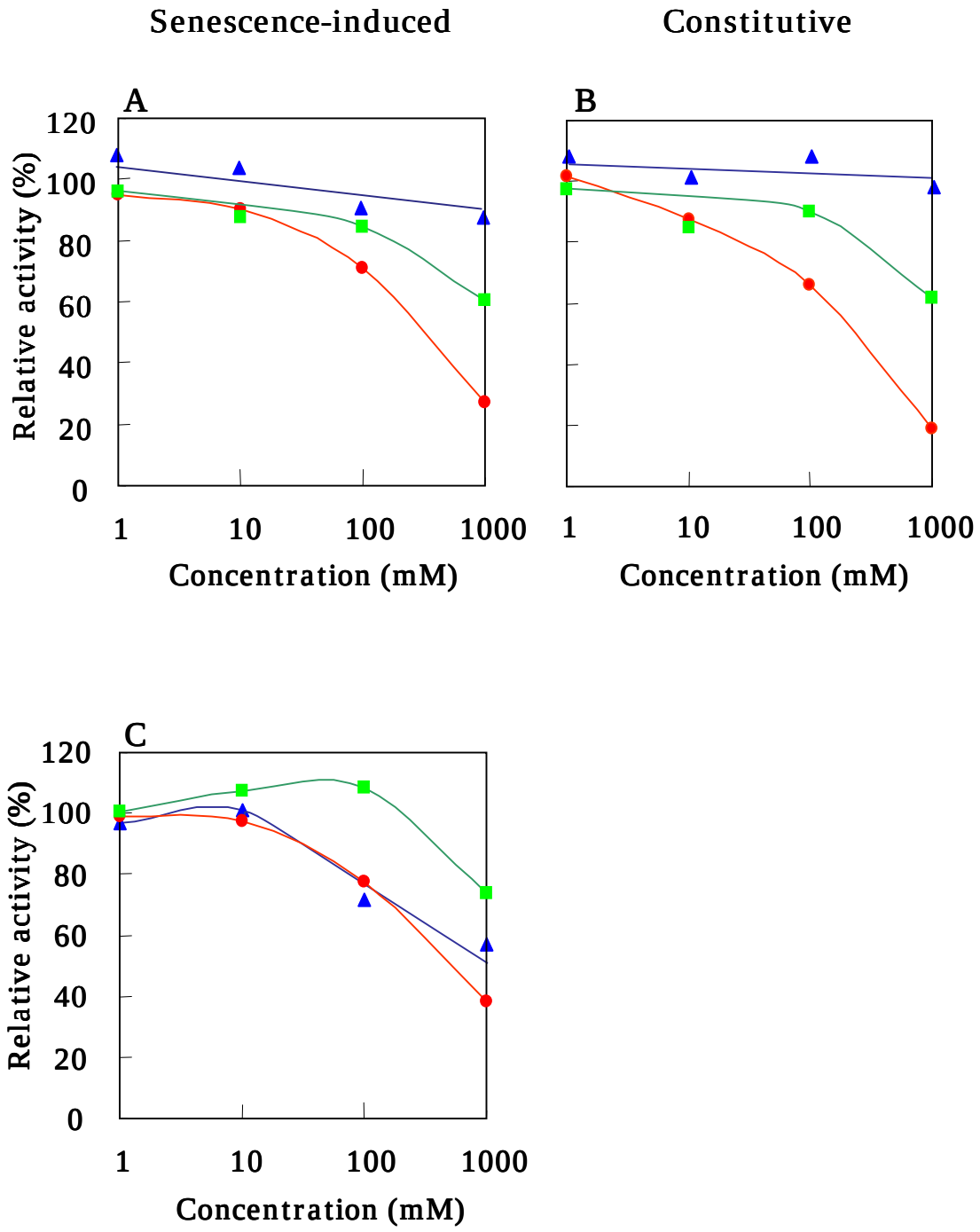

Fig. III-2. Effect of possible reaction products on the enzyme activity. Methanol, ethanol and methyl formate were used as reaction product analogues. Enzyme assays were carried out under the standard conditions described in Materials and Methods. Enzyme activity is expressed as relative percentages of that of 0 M alcohols. A, Phedase type 1; B, Phedase type 2; C, PDC. ●, methanol; ▲, ethanol; ■, methyl formate.

because acetone also inhibited the activity. Thus, inhibition of PDC activity by alcohols may be due to a simple inactivation of the enzyme. The addition of methyl formate made no difference between the two types of Phedases and PDC. These results suggest that the action of methanol differs between the Phedases and PDC, indicating a difference of the reaction mechanism of these enzymes.

In order to understand the reaction mechanism further, effects of various inhibitors on the enzyme activities were examined (Table III-2). Phedase is considered to be an esterase from its reaction mechanism. In fact, the activity of Phedase type 1 was decreased to 39% by a carboxyl esterase inhibitor, phenylmethylsulfonic fluoride (PMSF); however, Phedase type 2 had somewhat lower sensitivity to PMSF, and the inhibition of PDC by PMSF was almost the same in Phedase type 2. In contrast to PMSF, eberactone A, known as a non-toxic inhibitor of esterase, was less effective on Phedase and PDC. Phedases were almost unaffected by *N*-ethylmaleimide (NEM); however, PDC activity was strongly reduced to 24% in the presence of 1 mM NEM. These results imply that serine and cysteine residues are located in active sites of Phedase type 1 and PDC, respectively. EDTA, a chelator of bivalent metal ions, rather stimulated the Phedase and PDC activities, indicating that metal ions are not involved in these enzyme activities.

Distribution of Phedase and PDC in plants and algae

Distribution of the enzymes Phedase and PDC was studied in a variety of plants and algae (Table III-3). The extracts obtained from non-senescent plants and concentrated by ammonium sulfate fractionation between 30% and 70% saturation were used for enzyme assay. Among 23 species from 15 different families, Phedase activity was found in *Hypolepis punctata, Ch. album* (Shioi et al. 1996b) and some species of Brassicaceae. In *H. panctata*, the rate of conversion of the precursor, C-13^2-carboxylpyropheophorbide *a*, to PyroPheid *a* was high compared to those of other plant species under the same reaction conditions. At present, there is no information on the reason why

Table III-2. Effect of various inhibitors on the enzyme activity

Inhibitor	Concentration (mM)	Relative activity (%)		
		Phedase		PDC [a]
		type 1[a]	type 2[b]	
Control	—	100	100	100
Ebelactone A	5 (mg/l)	85.6	102.0	93.7
PMSF	1	38.9	73.6	74.1
NEM	1	89.0	96.4	24.4
EDTA	1	122.2	109.2	108.7

[a]Senescence-induced

[b]Constitutive

Table III-3. Distribution of Phedase and PDC in plants and algae

Family	Species	Phedase[1]	PDC[2]
Green algae			
Chlorophyceae	*Chlamydomonas reinhardtii*	—	100
Pterodophytes			
Equisetaceae	*Equisetum arvense*	—	—
Pteridaceae	*Hypolepis punctata*	+[3]	
Polypodiaceae	*Lepisorus thunbergianus*	—	—
Gymnosperms			
Ginkgoaceae	*Ginkgo biloba*	—	—
Angiosperms			
Chenopodiaceae	*Chenopodium album*	90	
	Spinacia oleracea	—	—
Polygonaceae	*Rumex acetosa*	—	
Theaceae	*Camellia sinensis*	—	
Tiliaceae	*Corcborus olitorius*	—	
Brassicaceae	*Raphanus sativus*	100	
	Rorippa nasturtiumaquaticum	178	
	Brassica napus	77	
	Brassica oleracea	21	
	Brassica campestris	49	
	Brassica chinensis	33	
	Brassica pekinensis	7.4	
	Arabidopsis thaliana	6.1	
Leguminosae	*Pisum sativum*	—	—
Labiatae	*Perilla frutescens*	—	
Composoitae	*Chrysanthemum coronarium*	—	
Umbelliferae	*Petroselinum sativum*	—	
Gramineae	*Hordeum vulgare*	—	—

[1]Phedase activity is expressed as percentages relative to that of *R. sativus.*

[2]PDC activity is expressed as percentages relative to that of *C. reinhardtii.*

[3]The rate of decarboxylation was too fast to measure exactly.

—: not detected.

Blank: not determined.

rapid conversion of the precursor occurs only in this plant, although an acceleration of decarboxylation reaction is largely dependent on conditions such as temperature and solvent concentration, as reported previously (Watanabe et al. 1995). To investigate the localization of Phedase in radish seedlings, the enzyme activity was measured in the extracts of leaf, stem and root. Phedase activity was detected only in leaves. Preliminarily, these enzymes were found to localize in the cytosol, consistent with the previous report for Phedase from *Ch. album* (Watanabe et al. 1999). PDC activity was not detected in the plants lacking Phedase activity, but was only detected in *C. reinhardtii* among species tested. PDC seems to be specific to algae.

Discussion

The accumulation of Pheid *a* derivatives has been reported in a variety of photosynthetic organisms (Matile et al. 1999; Takamiya et al. 2000). In this article, we describe two enzymes, Phedase and PDC, involved in the formation of PyroPheid and some properties of these enzymes. These enzymes have different reaction mechanisms based on the presence and absence of a biosynthetic intermediate. Phedase is considered to be an esterase and hydrolyzes Pheid *a* to yield methanol and C-13^2-carboxylpyropheophorbide *a*, followed by a non-enzymatic decarboxylation of the C-13^2-carboxyl-pyropheophorbide *a* to PyroPheid *a*. In the PDC reaction, however, the intermediate that appeared in the former Phedase was absent, and a nucleophilic reaction is proposed to form PyroPheid *a*. These reaction mechanisms were also corroborated by the results from the inhibitor study including the effect of the reaction product, methanol, on the activity of the purified Phedases and PDC (Fig. III-2). From these results, it is likely that two alternative pathways in the demethoxycarbonyl reaction of Pheid are catalyzed by different enzymes, Phedase and PDC.

PDC is not found in terrestrial plants as far as we know. This suggests

that PDC may only function in algae like *Chlamydomonas*, although there is limited information. Our recent analysis of the pigments in marine phytoplanktons showed that the accumulation of Pheid *a* and PyroPheid *a* is a common process throughout the year, although their amounts fluctuated. It would be interesting to know whether the activity of PDC is involved in the accumulation of PyroPheid *a* in these marine phytoplanktons. Further study on distribution of PDC, especially in algae, is needed.

There is little information concerning the demethoxycarbonylation reaction of C-13^2 position of Chls other than Pheid species including bacteriopheophorbide (BPheid) *a* (Haidl et al. 1985). When intact cells of *Euglena gracilis* were maintained in darkness, pyropheophytin *a* increase accompanied Phe *a* decrease (Schoch et al. 1981). Azuma et al. (1999) noted that the pathway of Chl catabolism in *Citrus* fruits is complex. In addition to PyroPheid formation by Phedase, they presume the possibility of pyrochlorophyllide *a* formation from the conversion of Chlid *a* in a similar manner as that reported for the Phedase reaction (Shioi et al. 1996b).

The purified Phedase and PDC were, however, specific for Pheid species of dihydro- and tetrahydroporphyrins such as BPheid *a*, but they could not use Phe *a* and Chlid *a* as substrates. These results suggest that the demethoxycarbonylation reaction may occur generally towards various Chl derivatives under natural conditions and that several enzymes specific for the different derivatives may be present and play a role. To clarify and understand this, purification of enzymes responsible for each reaction is necessary.

The main pathway of Chl degradation is considered to be catabolization via Pheid *a* to red Chl catabolite by the action of Pheid *a* oxygenase (Matile et al. 1999). Subsequently, nonfluorescent Chl catabolites (NCCs) are formed from red Chl catabolite. These are the first colorless tetrapyrrole products in the Chl degradation pathway, and their structure differs among plant species (Matile et al. 1999). In three NCCs from oilseed rape, the structure is

modified as the C-13^2 position is demethylated, but not demethoxycarbonylated. On the other hand, *Hv*-NCC-1 from barley leaves and *So*-NCC-2, a major NCC from spinach (Oberhuber et al. 2001) have an intact C-13^2-methoxycarbonyl group. These structures of the catabolites were consistent with the presence or absence of Phedase in these plant species.

In the green peel of *Citrus* fruits, PyroPheid *a* was present but gradually disappeared with ripening and was finally undetectable in the last harvest (Kurata et al. 1998). This further suggests that *Citrus* fruits accumulate PyroPheid *a* and contain its catabolic system. This implies that accumulated PyroPheid is also finally metabolized into colorless substances as Pheid is. We therefore must clarify whether PyroPheid *a* is a substrate for Pheid *a* oxygenase and whether a different pathway exists in the breakdown of PyroPheid *a*.

In the breakdown pathway of Chls, oxygen is necessary to open the Chl macrocyclic ring. When the oxygen supply is suppressed or limited, destruction of Pheid *a* does not occur; instead, PyroPheid *a* accumulation occurs, as is evident in mutant cells of *C. reinhardtii* under anaerobiosis (Doi et al. 2001). Furthermore, the acceleration of PyroPheid *a* formation was observed under anaerobic conditions *in vivo*. Thus, accumulation of PyroPheid *a* occurs temporally before its final degradation. It is also assumed that PyroPheid accumulation to a certain level might act as a signal, and rapid Chl degradation could start via cleavage of macrocyclic ring of Chls to low molecular components like monopyrrole derivatives that are likely to be recycled from senescent cells to other parts of tissues or organs in the plant (Suzuki and Shioi 1999).

Interestingly, the accumulation of Chl degradation products by a red Chl catabolite reductase mutant of *Arabidopsis thaliana* could spontaneously cause spreading cell death (Mach et al. 2001). If this is the case, the regulation of cell death by accumulation of PyroPheid *a* by auxiliary reaction should be considered. Further investigation of the regulation of cell death by degradation products would be worthwhile to understand this process in

plants.

In conclusion, there are at least two alternative pathways in the demethoxycarbonyl reaction of Pheid that catalyze by different enzymes, Phedase and PDC.

Chapter IV

Purification and Cloning of Pyropheophorbide Forming Enzyme, Pheophorbidase, from *Raphanus sativus*

Introduction

Chlorophylls (Chls) are degraded through the several steps of reactions catalyzed by enzymes as shown in Chapter I. About half of enzymes, which involves in those reactions, are characterized. Until now, cloning of genes is only performed on chlorophyllase (Chlase) and red Chl catabolite (RCC) reductase (RCCR).

Chlase is considered to involve in the first step of Chl degradation, and had been confronted by many investigators for long years. Although the activity of Chlase has been revealed 90 years ago (Willstätter and Stoll 1913), molecular cloning of its gene was accomplished recently. Tsuchiya et al. (1999) and Jacob-Wilk et al. (1999) cloned cDNA encoding Chlase independently from *Chenopodium album* and *Citrus sinensis*, respectively. On the other hand, Benedetti et al. (1998) reported *ATHCOR1* as coronatine-induced gene by differential display from *Arabidopsis thaliana.* However, the function of the protein encoded had not been elucidated. From the results of homology searching with their sequences and expression during study on Chlase from *A. thaliana* (Tsuchiya et al. 1999), *ATHCOR1* is identified to be the gene encoding Chlase. More recently, Benedetti and Arruda (2002) confirmed the fact that in vivo activity of the protein encoded *ATHCOR1,* it was Chlase from the study on mutant, which lacks *ATHCOR1* transcripts, and transgenic *A. thaliana* that transformed with sense and antisense *ATHCOR1.* In 2003, Tsuchiya et al. (2003) demonstrated that three amino acid residues were essential for Chlase activity and they also proposed a plausible catalytic mechanism for this enzyme by analysis of site-directed mutagenesis with Chlase from *C. album*.

RCCR is the enzyme that catalyzes the formation of a primary fluorescent catabolite from macrocyclic-cleavaged pheophorbide (Pheid), RCC. RCCR was cloned from *Hordeum vulgare* and *A. thaliana* (Wüthrich et al. 2000). Interestingly, *Accelerated Cell Death 2 (ACD2)* gene, which causes lesion mimic by mutant *acd,* was revealed to encode the *A. thaliana* homologue of RCCR (Mach et al. 2001). *ACD2* was cloned by the investigation on hypersensitive

response. This is suggested the possibility that breakdown products of Chl may involve in the hypersensitive response.

Pheophorbidase (Phedase) is an enzyme considered to be the final step of the macrocyclic-modification stage and catalyzes the formation of C-13^2-carboxylpyropheophorbide *a* from Pheid *a* (Shioi et al. 1996b). We reported that Phedase consisted of senescence-induced (type 1) and constitutive (type 2) types and that the activity of Phedase was specific for plant species (Suzuki and Shioi, 2001; Suzuki et al., 2002). Previously, Phedase of *C. album* was purified and N-terminal sequences were determined (Watanabe et al. 1999). There is, however, a little information concerning molecular structure including gene cloning.

In this Chapter, we highly purified two types of Phedase from the senescent cotyledons of *R. sativus* and determined N-terminal and internal amino acid sequences and also a cDNA sequence. Molecular structure of Phedase, especially molecular mass and subunit structure, are discussed in light of 3D domain swapping theory.

Materials and Methods

Plant materials

Cotyledons of radish (*Raphanus sativus* L.) were purchased from a local market. Induction of senescence was performed according to the method described previously (Suzuki and Shioi 1999). Shoots were excised and placed in 50-ml flasks containing 15 ml distilled water. The cotyledons were allowed to reach senescence in complete darkness at 25°C.

Chlorophylls

Chl *a*, Pheid *a* and pyropheophorbide (PyroPheid) *a* were purchased from Wako Pure Chemical Industries (Osaka, Japan). Chlorophyllide (Chlid) *a* was prepared from Chl *a* by enzymatic reaction using a Chlase (EC 3.1.1.14.)

prepared from *Chenopodium album* (Tsuchiya et al. 1997). The concentrations of Pheid *a* and PyroPheid *a* were determined spectrophotometrically as described previously (Doi et al. 1997).

Enzyme assay

The activity of Phedases was assayed basically according to the methods described by Shioi et al. (1996b). The reaction mixture consisted of 20 mM phosphate buffer (pH 7.0), 160 μM Pheid *a* in acetone (final 20%, v/v) acetone and Phedase preparation in a total volume of 100 μl. After incubation in darkness at 30°C for 10 min, the reaction was terminated by adding 200 μl acetone. The amount of C-13^2-carboxylpyropheophorbide *a* formed was assayed using the HPLC system described below.

HPLC analysis of the pigments was carried out according to our previous method with a slight modification (Shioi et al. 1996b). Briefly, HPLC was performed using a Zorbax ODS column (250 x 4.6 mm) (Agilent Technologies, Inc., CA, USA) or Cosmosil 5C18-MS Column (250 x 4.6 mm) (Nacalai tesque, Kyoto, Japan). Pigments were eluted isocratically with methanol-2 M ammonium acetate (95/5, v/v) at a flow rate of 1.0 ml per min at 30°C. The pigments were monitored spectrophotometrically at 410 nm and quantified by an integrator. Peak areas were used for the calculation of the enzyme activity. Concentration of C-13^2-carboxylpyropheophorbide *a* was tentatively calculated using the standard curve for PyroPheid *a,* since isolated C-13^2-carboxyl-pyropheophorbide *a* rapidly changed to PyroPheid *a* spontaneously (Shioi et al. 1996b)

Purification of Phedase

Senescent cotyledons of radish (ca. 5,000 g) were homogenized with 20 mM phosphate buffer (pH 7.0) at 4°C in a blender. The homogenate was filtered through six layers of cotton gauze and centrifuged at 17,000 x g for 30 min at 4°C. The cell-free extract was incubated at 60°C for 10 min and

centrifuged 12,000 x g for 15 min. The supernatant was fractionated with 60% acetone. The precipitate was dissolved in a small volume of 20 mM Tris-HCl (pH 7.5). The enzyme solution was applied to a column of DEAE-Toyopearl 650M (2.5 x 8 cm) (Tosoh, Tokyo, Japan) previously equilibrated with 20 mM Tris-HCl (pH 7.5) and eluted with the same buffer containing a linear gradient of NaCl (0-0.35 M). Fractions eluted about 0.1-0.14M NaCl as senescence-induced (type 1) and 0.15-0.2 M as constitutive (type 2) were pooled (see Fig. IV-1). The following purification procedures were carried out separately. After adding ammonium sulfate to 30% saturation, the enzyme solution was applied to a Butyl-Toyopearl column 650M (2.5 x 8 cm) (Tosoh) previously equilibrated with 20 mM Tris-HCl (pH 7.5) containing 30% saturation of ammonium sulfate and eluted with the same buffer containing a reverse-linear gradient of ammonium sulfate (30-0% saturation). Fractions eluted about 0-6% saturation for type 1 and 6-12% saturation for type 2 were pooled. The active fraction was dialyzed against 20 mM Tris-HCl (pH 7.2) and charged onto a column of Mono-Q (Amersham Pharmacia Biotech, Uppsala, Sweden) which had been equilibrated with the same buffer using ÄKTA*FPLC* system (Amersham Pharmacia Biotech). The column was eluted with the same buffer containing a linear gradient of NaCl (0-0.45 M). The pooled enzyme solution was concentrated by Centriflo® CF25 Membrane Cones (Millipore, MA, USA) and applied to a column of Superdex 200 (Amersham Pharmacia Biotech) equilibrated with 20 mM Tris-HCl (pH 7.5) containing 0.15 M NaCl and eluted with the same buffer. Active fractions were collected and used for subsequent experiments.

Protein determination

Protein concentrations were determined using a BCA Protein Assay Kit (Pierce, IL, USA) with bovine serum albumin as a standard.

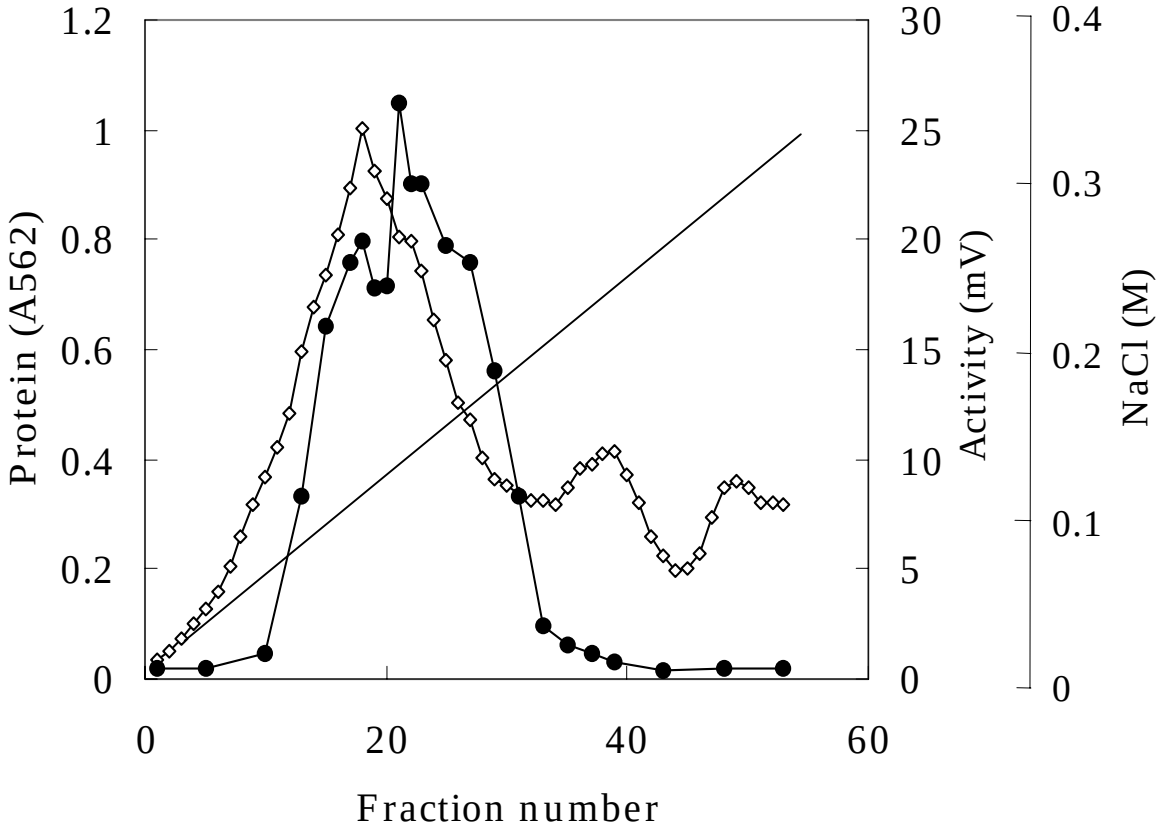

Fig. IV-1. Elution profile of DEAE-Toyopearl chromatography of Phedase that correspond to about 500 g of radish cotyledons. The column was equilibrated with 20 mM Tris-HCl buffer (pH 7.5) and eluted with the same buffer containing a linear gradient of NaCl (0-0.35 M) at a flow rate of 1 ml per min. The fractions of 3 ml were collected. Phedase activity is presented by the value of peak area detected by HPLC. ◇, Protein concentrations estimated by BCA method with absorbance at 562 nm; ●, Phedase activity; —, NaCl concentration. Front peak of activity emerged in senescence-induced cotyledons and back one existed constitutively. Each fraction was designated type 1 and type 2 by the order of elution.

Electrophoresis

SDS-PAGE was performed by the method of Laemmli (1970) using 15% or 12% polyacrylamide gel under reducing conditions. Heat treatment was performed at ca. 95°C for 1 to 20 min. Fixing and staining were done in aqueous methanol (25%, v/v) containing acetic acid (7.5%, v/v) and Coomassie Brilliant Blue R-250. Then gel was destained with aqueous 25% methanol containing 7.5% acetic acid until the bands emerged.

Preparation of substrates

Chls *a* and *b* were extracted from the leaves of spinach (*Spinacia oleracea*) with acetone and were partially purified by precipitation with dioxane (Iriyama et al. 1974). The dioxane-precipitation was repeated once and Chls obtained were separated and further purified by sucrose-column chromatography (Perkins and Roberts 1962). Bacteriochlorophyll (BChl) *a* was extracted from the cells of *Rhodobacter sulfidophilus*. Protochlorophyllide (PChlid) *a* was obtained from 6-day-old etiolated leaves of barley with acetone. Chl *c* (c_1 and c_2 mixture) was extracted from the thalli of *Undaria pinnatifida*. Pheophytins (Phes) *a* and *c*, Pheid *b* and bacteriopheophorbide (BPheid) *a* were prepared by acid treatment of pure respective Chls, according to the method of Perkins and Roberts (1962) and Hynninen (1973).

Chlid species were prepared from pure respective Chls by action of Chlase which catalyzes the hydrolysis of esterified alcohols. Chlase was obtained from mature leaves of *C. album* as described previously (Tsuchiya et al. 1997).

Each pigment was purified further by DEAE-Toyopearl (acetate form) chromatography (Omata and Murata, 1980) or by sucrose-column chromatography.

Analysis of the N-terminal amino acid sequence

Purified Phedase was electrophoresed on a 15% SDS-polyacrylamide gel and electrotransferred to polyvinylidene difluoride membrane. The protein

bands visualized with Coomassie Brilliant Blue were cut out and subjected to amino acid sequencing on a protein sequencer PPSQ-21A (Shimadzu, Kyoto, Japan).

BLAST searching

The analogous genomic and amino acidic sequence of Phedase were obtained by searching against non-redundant (nr) NCBI databases (http://www.ncbi.nlm.nih.gov/BLAST/), TAIR BLAST 2.0 (http://www.arabidopsis.org/Blast/), *Chlamydomonas reinhardtii* EST Index of Kazusa DNA Research Institute (http://www.kazusa.or.jp/en/plant/chlamy/EST/) and CyanoBase (http://www.kazusa.or.jp/cyano/cyano.html).

RNA extraction

Total RNA was isolated from 1-day-senescent cotyledons of radish by the guanidinium thiocyanate method (Chomczynski and Sacchi, 1987). Total RNA concentrations were determined by UV spectrophotometry.

Reverse transcriptase-PCR (RT-PCR)

For RT-PCR (Frohman et al. 1988), cDNA synthesis was performed using a ReverTra Ace -α-^{R} (Toyobo, Osaka, Japan) from total RNA isolated from senescent radish leaves, according to the manufacturer's instructions. Based on the partial amino acid sequences, degenerate primers were designed as follows: a forward primer, 5'-CAYTTYGTNTTYGTNCAYGGNGC-3' and a reverse primer, 5'-ATRTAYTCCCTDATRTCYTCYTC-3', where D indicates not C, N indicates any, R indicates purines (G + A), and Y indicates pyrimidines (T + C). A partial cDNA (375 bp) was amplified using *TaKaRa Taq*™ (Takara, Shiga, Japan) with primers for 40 cycles at 97°C for 0.5 min, 47°C and 72°C for each 1 min. The PCR products were cloned into pT7-Blue T-Vector (Novagen, WI, USA) and sequenced.

Rapid amplification of cDNA ends (RACE)

For 3'-RACE, total RNA from radish was used as a template with oligo d(T) primer to produce single-strand cDNA. Based on the results of RT-PCR, sequence-specific primers were designed as follows: 5'-GGTATCAACCTCACCGACTCTAA-3'. A partial cDNA (550 bp) was amplified using *TaKaRa Taq*™ with sequence-specific primer and oligo d(T) for 40 cycles at 97°C for 0.5 min, 60°C and 72°C for each 1 min.

Results

Purification

The crude enzyme, extracted from 4,937 g (fresh weight) of cotyledons of radish, was purified by four steps of successive chromatography (Table IV-1). The enzyme activity was separated into two peaks in the chromatography of DEAE-Toyopearl and Butyl-Toyopearl. Phedases were termed type 1 and type 2, according to their order of elution in DEAE-Toyopearl chromatography (Fig. IV-1). Type 1 appeared only after senescence, indicating that type 1 Phedase is induced by senescence and type 2 enzyme is constitutive. These enzymes were purified separately in the following chromatography. Phedase types 1 and 2 were purified 9,999 and 6,476-fold with a yield of 0.703% and 2.73%, respectively. The summary of purification of two Phedases is presented in Table IV-1. Some enzymatic properties, for example, pH optimum and the effect of reaction products, were shown in previously (Suzuki et al. 2002).

SDS-PAGE was performed with purified Phedase type 2 (Fig. IV-2). In non-heat treatment samples, one major band whose size was about 77 kDa appeared in 15% polyacrylamide gel (lane 1), while on 12% gel, a single band emerged at the size of 61.3 kDa. Even after one min of heat-treatment of the enzyme with sample buffer containg SDS and 2-mercaptoethanol, the Phedase was separated into three bands with molecular mass of 16.8, 15.9 and 11.8 kDa (lane 2). The pattern of SDS-PAGE was not changed after heating for 1 to

Table IV-1. Purification of Phedase from cotyledons of *R. sativus*

Purification step	Protein (mg)	Total activity (mV·ml)	Specific activity (mV·ml/mg protein)	Yield (%)	Purification (-fold)
Crude	121940	129220	1.060	100	1
Heat treatment	110675	120350	1.087	93.1	1.03
Acetone fractionation	3255	39041	11.99	30.2	11.3
Type 1					
DEAE Toyopearl	163.9	32299	197.1	25.0	186
Butyl Toyopearl	7.483	14930	1995	11.6	1883
Mono Q	0.6890	2232	3239	1.73	3057
Superdex 200	0.08568	907.9	10597	0.703	9999
Type 2					
DEAE Toyopearl	126.6	22219	175.5	17.2	166
Butyl Toyopearl	26.94	18694	693.9	14.5	655
Mono Q	1.362	8844	6493	6.84	6128
Superdex 200	0.5145	3531	6863	2.73	6476

Purification was started from 4,937 g fresh weight.

mV is the value of peak area detected by HPLC.

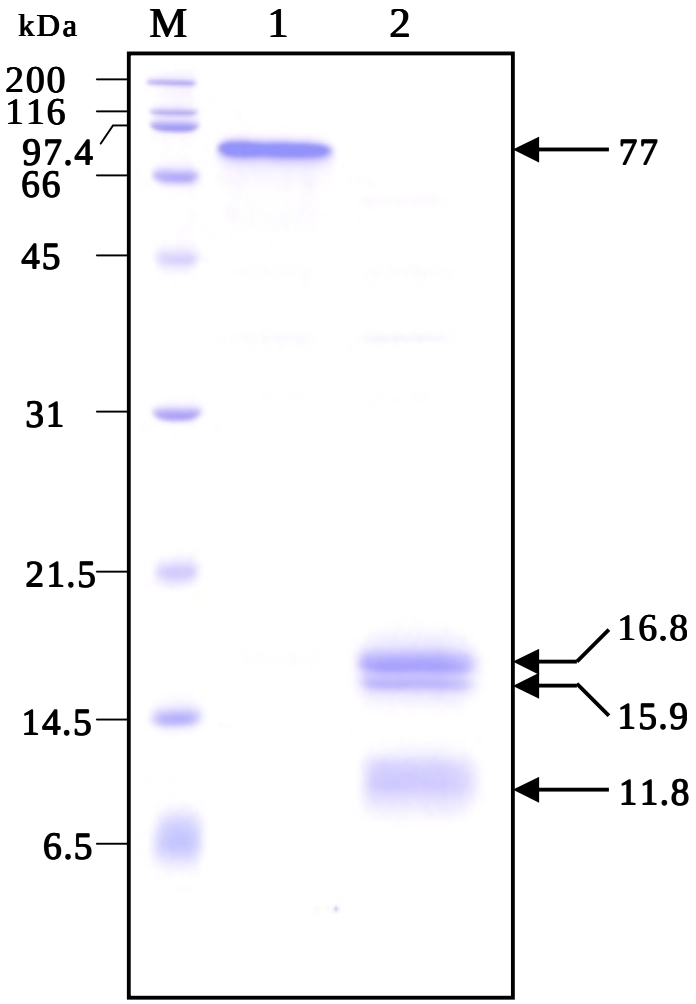

Fig. IV-2. SDS-PAGE on 15% polyacrylamide gel of purified Phedase (type 2) from *R. sativus.* Peptides were stained by Coomassie brilliant blue R-250. In non-heating sample (lane 1), only one band was stained. After heating at 95ºC for 3 min (lane 2), Phedase was separated into three bands. Numerals under kDa denote the molecular masses of marker protein. Lane M , Molecular markers.

20 min. Similar results were also obtained in Phedase type 1.

Substrate specificity

The K_m for Pheid *a* of the two enzymes was determined in the concentration range from 1 to 40 μM. The values obtained were 14.1 μM and 15.1 μM for types 1 and 2, respectively (Table. IV-2).

To determine the substrate specificity of the enzyme, several derivatives of Chls were examined under the standard assay conditions. As shown in Table 2, both enzymes used Pheids *a* and *b* and BPheid *a* as the substrates, but not other Chl derivatives such as PChlid *a*, Phe *c*, Chls *a* and *b*, Chlid *a*, Phe *a*, and BChl *a*. These results indicate that the enzymes are specific for the structure of substrate, for instance, absence of Mg and phytol chain, and also existence of a single bond at a position of C-17-C-18.

For other substrates, the K_m values of two enzymes were also calculated to be about 240 μM and 40 μM for Pheid *b* and BPheid *a*, respectively. The K_m value for Pheid *b* was the highest among three Pheid species, suggesting that structures of Pheid *a* type were shown to have a greater affinity than *b* type.

Identification of the N-terminal sequence

The analyses of N-terminal sequences were performed with the three peptides separated by SDS-PAGE after heat treatment of the purified Phedase type 2. The amino acid sequences of each peptide were determined to be as follows: 16.8 kDa, EEDIWEYIYGEGADKPPTGVLMKEEFFRRY; 15.9 kDa, EDIWEYIYGEGADKPPTGVLMKEEFFRHYY; and 11.8 kDa, GDDSVVHFVFFHGASHGAAWYYKPTTTLVR. Only one amino acid of N-terminal sequence of 15.9 kDa lacked from that of 16.8 kDa, although C-terminus is uncertain. Thus, two separate partial amino acid sequences were revealed from this analysis.

BLAST searching (Alstchul et al. 1997) was performed against NCBI databases with two amino acid sequences. The results showed that the

Table IV-2. Substrate specificity of Phedase from *R. sativus.*

Chlorophyll species	Metal (Mg)	C-position C-17[a]	C-7	C-17-C-18 [b]	C-7-C-8[b]	K_m (μM)	
Porphyrins							
Protochlorophyllide *a*	+	propionyl	CH_3	double	double	–	–
Protopheophorbide *a*	–	propionyl	CH_3	double	double	–	–
Pheophytin *c*	–	acryl	CH_3	double	double	–	–
Dihydroporphyrins							
Chlorophyll *a*	+	phytyl	CH_3	single	double	–	–
Chlorophyll *b*	+	phytyl	CHO	single	double	–	–
Chlorophyllide *a*	+	propionyl	CH_3	single	double	–	–
Pheophytin *a*	–	phytyl	CH_3	single	double	–	–
Pheophorbide *a*	–	propionyl	CH_3	single	double	14	15
Pheophorbide *a*'	–	propionyl	CH_3	single	double	–	–
Pheophorbide *b*	–	propionyl	CHO	single	double	243	232
Tetrahydroporphyrins							
Bacteriochlorophyll *a*	+	phytyl	CH_3	single	single	–	–
Bacteriopheophorbide *a*	–	propionyl	CH_3	single	single	39	37

[a]phytyl, $-CH_2-CH_2-COOC_{20}H_{30}$; propionyl, $-CH_2-CH_2-COOH$; acryl, $-CH=CH-COOH$

[b]single, single bond; double, double bond

protein, NP_193402, of *Arabidopsis thaliana* had high homology of 77% and 64% to Phedase peptides. The details of NP_193402 are mentioned below. From the comparison with NP_193402, amino acid sequence of 11.8 kDa located upstream from those of 16.8 and 15.9 kDa. Sense and antisense degenerate primers were, therefore, designed from the amino acid sequence of Phedase constructed according to the sequences of 11.8 and 16.8 kDa peptides.

Cloning of cDNA for Phedase

cDNA fragment of 862 bp with the termination codon TGA at position 754 was cloned by a combination of RT-PCR and 3'-RACE from *R. sativus* RNA (Fig. IV-3). The amino acid sequence deduced from the nucleic acid sequence was 251 amino acid residues. The deduced polypeptide had lipase domain that was presumed to be an active site of esterases as well as Chlase (Tsuchiya et al. 2003). Some positions of base pair could not determine to be one nucleotide. The fluctuation of positions 340, 346 and 351 caused the difference of encoding amino acid, Asp or Thr, Ile or Val, and Ile or Met, respectively.

Deduced Phedase Sequence and its homologues

Homology searching against the deduced amino acid sequence of Phedase was performed with BLAST programs using NCBI databases and TAIR BLAST 2.0. From the results of homology search, two homologues highly conserved, NP_193402 from *A. thaliana* (GI: 15235844) and CAC82615 from *Capsella rubella* (GI: 15866583), were found. The multiple alignment of the deduced Phedase sequence and its homologues using ClustalW (Higgins et al. 1996) is shown in Fig. IV-4. NP_193402 is "cyanohydrin lyase like protein" of *A. thaliana* and consisted of 262 amino acids (MW = 28,996). The gene of NP_193402, At4g16690, locates at chromosome 4 of *A. thaliana* and contains two introns. CAC82615 is "hypothetical protein" of *C. rubella* and consisted of 265 amino acids (MW = 29,347). NP_193402 and CAC82615 had high level of amino acid sequence conservation to the deduced amino acid of Phedase to 84%

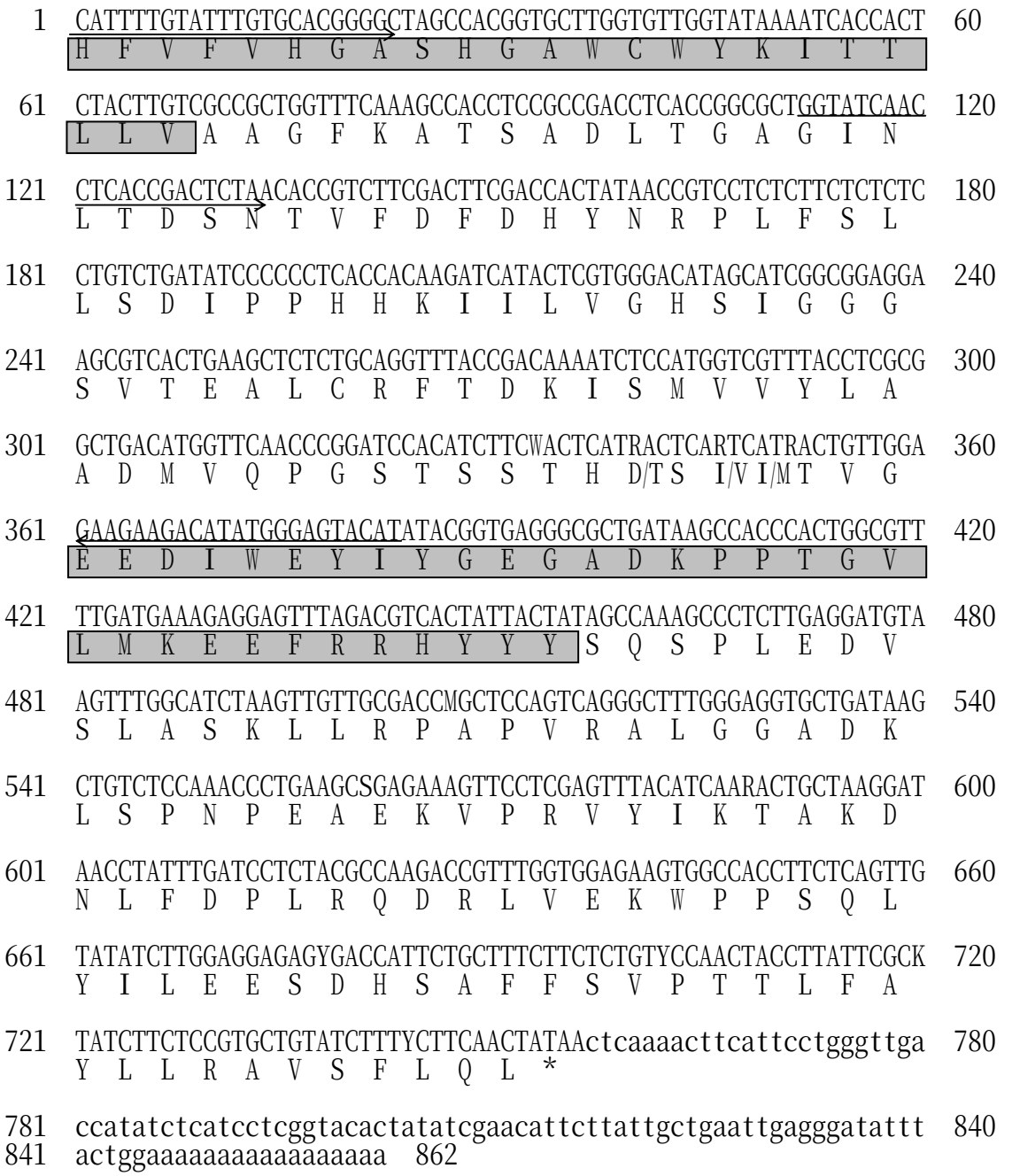

Fig. IV-3. Partial nucleotide sequence of cDNA encoding Phedase of *R. sativus*. The deduced amino acid sequence is denoted below in the standard one-letter code. The translation termination codon is designated with an asterisk (*). Gray boxes indicate the results of N-terminal sequences analyses. All PCR primers used in the present study are shown arrows.

Fig. IV-4. Comparison of amino acid sequences among Phedases form *R. sativus* and the homologues. Homology searching was performed with BLAST programs. The alignments of the sequences were obtained using ClustalW. The lipase domain is shown with underlined. Arrowhead indicates the position that cleaved by heating at 95°C. NP_193402, *A. thaliana* (GI: 15235844); CAC82615, *Capsella rubella* (GI: 15866583).

and 77% identity, respectively. All peptides have lipase domain (Hasslachar et al. 1995) whose pattern is [LIV]-x-[LIVFY]-[LIVMST]-G-[HYWV]-S-x-G-[GSTAC] (underlined in Fig. IV-4). When the amino acid sequences of Phedase and NP_193402 were aligned with CAC82615, it was found that Phedase and NP_193402 have gaps. In particular, the gap shown arrowhead in Fig. IV-4 corresponds to the cleaved position of Phedase by heating as shown in SDS-PAGE (Fig. IV-3, lane 2). Subsequently, homologues of Phedase were searched against *C. reinhardtii* EST Index of Kazusa DNA Research Institute, because *C. reinhardtii* had an enzyme, which catalyzes the conversion of Pheid to PyroPheid. No homologues were, however, found in *C. reinhardtii* EST and also in CyanoBase.

Discussion

In Chl degradation, reaction pathway is operationally divided into three stages (Fig. I-1). The early stage includes modifications of the side chain of tetrapyrrole macrocycle and isocyclic ring. The middle stage involves cleavage of macrocyclic ring and successive modifications. The late stage is subsequent degradation of open tetrapyrroles to smaller carbon and nitrogen containing fragments like organic acids as shown Chapter V.

In the final step of the early stage, it has been shown that there are two reactions involved in the formation of PyroPheid from Pheid (Shioi et al. 1996b). The enzyme, which catalyzes the hydrolysis of Pheid to yield precursor of PyroPheid, was designated “Pheophorbidase (Phedase)”. The purification and enzymic properties of Phedases have been reported from mature leaves of *C. album* (Shioi et al. 1996b; Watanabe et al. 1999) and cotyledons of *R. sativus* (Suzuki et al. 2002). We operationally named Phedases by prefix their species name to distinguish the sources, i.e., RsPhedase for Phedase from *R. sativus* and CaPhedase from *C. album*. We previously discovered that RsPhedase is composed of two types, senescence-induced and constitutive enzymes. In the

present study, two RsPhedases were highly purified from *R. sativus* and determined their partial amino acid sequences and a cDNA sequence with RT-PCR and RACE.

The pathway of Chl degradation was considered to exist only in thylakoids and innerenvelope membranes (Matile et al. 1999). However, recent results suggest the possibility that Chl is degraded both in inside and outside of chloroplast. Since, Chlase has a signal peptide for endoplasmic reticulum in addition to a transit peptide for plastid (Tsuchiya et al. 1999). In the case of Phedase, it is confirmed that CaPhedase is located outside the chloroplast in *C. album* (Watanabe et al. 1999). RsPhedase and its homologues were analyzed based on amino acid sequences using SOSUI system (http://sosui.proteome.bio.tuat.ac.jp/cgi-bin/sosui.cgi?/sosui_submit.html) whether they are membrane protein or not. RsPhedase and its homologues were estimated to be soluble proteins. The putative cleavage site of the signal peptide was analyzed by the PSORT prediction (http://psort.nibb.ac.jp/), and 14 amino acids at N-terminus seemed to be a signal sequence for vacuole. In practice, however, RsPhedase had not been cleaved at this position. It is expected that RsPhedase have not signal sequence, because the cleavage site was different from the result of N-terminal sequence analysis. The putative cleavage site was also predicted against NP_193402, the RsPhedase homologue from *A. thaliana*. However, NP_193402 seemed to have not N-terminal signal sequence.

There are several similarities in molecular structure between RsPhedase and CaPhedase. Twenty residues of N-terminal amino acid sequences of CaPhedase had been determined (Watanabe et al. 1999). Among those peptide sequences of CaPhedase, 11 amino acid residues coincided with those of the deduced sequence of RsPhedase. The molecular weight of Phedase was determined by gel filtration chromatography to be 113,000 for RsPhedase (Suzuki et al. 2002) and 105,000 for CaPhedase (Watanabe et al. 1999). Consequently, molecular weight was similar between RsPhedases and

CaPhedase, although the size obtained from denatured electrophoresis was different.

One major band whose size is about 77 kDa appeared in denatured 15% PAGE of RsPhedase using non-heat treatment after mixed with sample buffer containing SDS and 2-mercaptoethanol (Fig. IV-2, lane 1). Moreover, the molecular weight estimated from the deduced amino acid was about 28,000 and 113,000 by gel filtration chromatography, indicating that RsPhedase is homo-tetramer. The peptide of 77 kDa seems to be kept dimeric form. It is further suggested that RsPhedase might have strong stuck dimer. Molecular mass of RsPhedase is close to the band size of CaPhedase in the denatured electrophoresis. After heat treatment of RsPhedase, three bands, 16.8, 15.9 and 11.8 kDa, appeared by SDS-PAGE, but 16.8 and 15.9 kDa peptides overlapped in terms of the amino acid sequences. Excluding the overlapped peptide, the sum of molecular mass of the rest bands was 28.6 kDa. The sizes of deduced peptide fragments, N-terminal and C-terminal fragments, from cleavage site (Fig. IV-4, arrowhead) were 12,800 and 15,100, respectively, corresponding to the approximate band sizes. As shown in Fig. IV-4, RsPhedase cleaved at non-conservative amino acid site (gap structure). Based on the tough dimer form and the fragile primary structure, we postulate that RsPhedase forms into dimer by 3D domain swapping (Jaskólski 2001). First, 3D domain swapping was established by X-ray crystallography in diphtheria toxin (Bennett et al. 1994). In 3D domain swapping, a structural element of a monomeric protein is replaced by same element from another subunit. The main adhesive force allowing the domain-swapped oligomer of form is the “closed interface” between the swapped domains, which recreates the structure and interactions of the protomer. It is a powerful factor in the structure of the oligomer as it has evolved to provide stability of the monomeric molecule. The hinge regions in new conformation form a new intermolecular interface that was not present in the monomer. In some case, hinge region is opened. In a protein capable of undergoing domain swapping, there must exist a flexible

linker or hinge region. This hypothesis is able to explain the formation of the new dimer by displacement and deficiency of a few amino acids. From the results of prediction for secondary structure of RsPhedase and the homologues by New Joint Method (PAPIA: http://www.cbrc.jp/papia-cgi/ssp_queryJ.pl?query=seq), cleavage site was assumed to form coil structure, however information about domain structure was not obtained. To elucidate the mechanism of shaping tertiary structure further, the structural analysis of RsPhedase is necessary.

Chapter V

HPLC Analysis of Products in the Late Stage of Chlorophyll Degradation in the Senescent Leaves of *Raphanus sativus* and *Hordeum vulgare*

Introduction

The main catabolites of degraded Chls after the cleavage of macrocyclic ring systems were identified as derivatives of bilin (Engel et al. 1991; Kräutler et al. 1991; Mühlecker et al. 1993; Iturraspe and Moyano. 1995; Doi et al. 1997). The accumulation of these derivatives has been reported in senescent leaves of several higher plants (Kräutler et al. 1991; Mühlecker et al. 1993; Iturraspe and Moyano1995) and algae (Engel et al. 1991; Doi et al. 1997). However, little is known about the subsequent reactions involved in the breakdown of these derivatives into low molecular weight compounds, except for the studies on the products of photodegradation of bilirubin and Chls. In the photodegradation of bilirubin, three groups of more than 10 species of products have been reported (Lightner 1977). These include dipyrroles, monopyrroles and their hydrolytic products. With respect to Chls, methyl ethyl maleimide (MEM) has previously been found in the photo-bleached endproduct of Chl dissolved in solvents (Jen and Mackinney 1970). The formation of several hydrophilic colorless products, low molecular weight organic acids, was measured in Chl *a* adsorbed on lipophilic particles during photodegradation (Llewellyn et al. 1990a, 1990b).

To elucidate the intermediary degradation step of Chls, we required a simple and rapid method for the separation and identification of degradation products of bilin derivatives, especially for monopyrrole derivatives. We, therefore, prepared putative catabolites of Chl, monopyrrole derivatives from Chl, and porphyrin, by oxidation with chromic acid according to the established method that has been used to determine the structure of bile pigments (Rüdiger 1968, 1969) (Fig. V-1).

In this Chapter V, we describe a chromatographic method using a wide pore ODP column which enables the separation of ethyl and vinyl species of maleimide in addition to hematinic acid (HA) and C-E-ring derivative of Chl by a rather simple isocratic elution system with a buffered mobile phase. Using this method, the intermediary breakdown products of Chls in senescent leaves

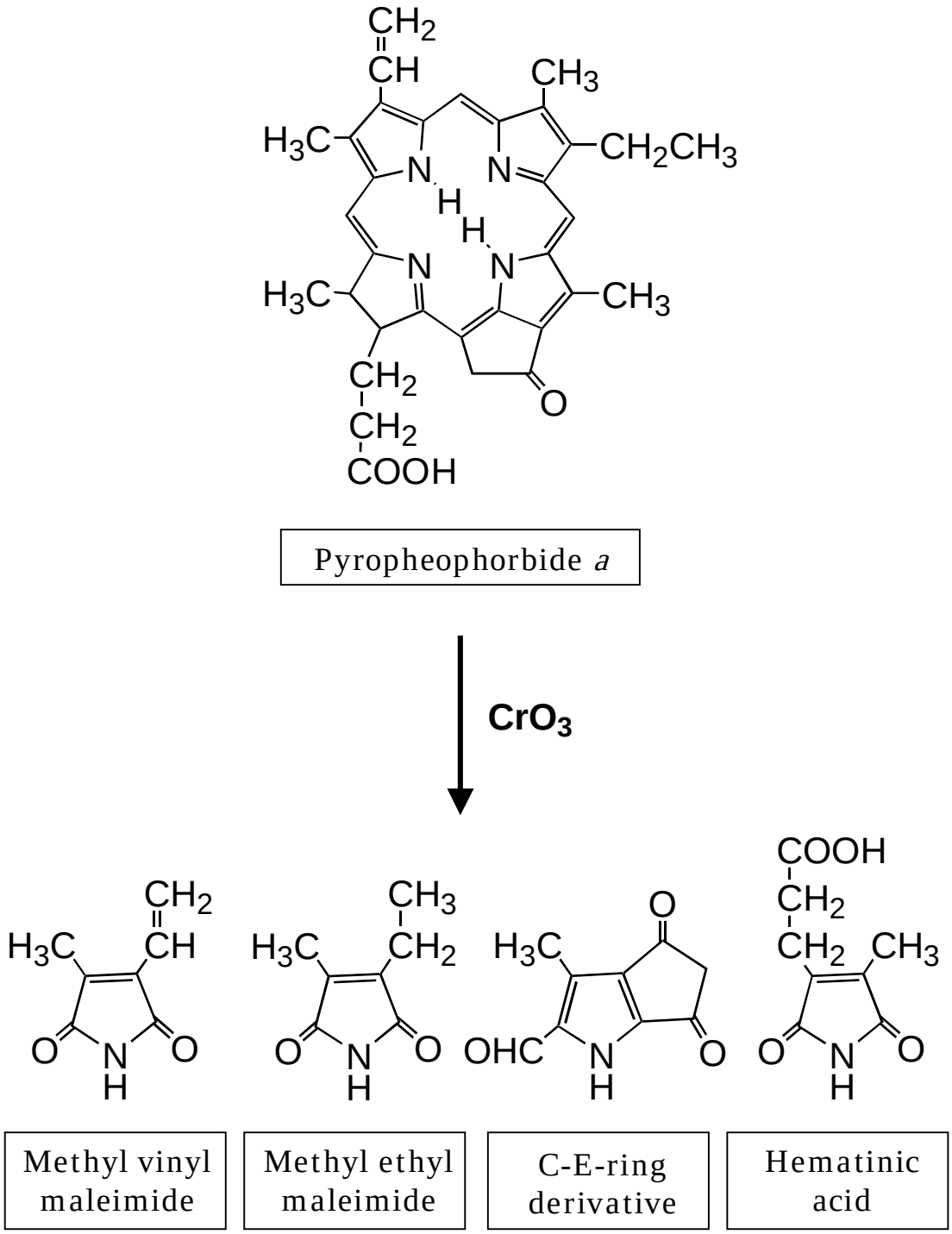

Fig. V-1. Structures of degradation products of pyropheophorbide *a* by oxidation with chromic acid. Four compounds, methyl vinyl maleimide, methyl ethyl maleimide, C-E-ring derivative, and hematinic acid are primarily formed.

of higher plants were determined (Suzuki et al. 1999). The results show that the degradation process and amounts of breakdown products of Chl depend largely on plant species and vary with length of senescence. The intermediary degradation step of Chl breakdown is discussed in terms of the appearance of the degradation products (Suzuki and Shioi 1999).

Materials and Methods

Chls and porphyrins

Pheophrobide (Pheid) *a* and pyropheophorbide (PyroPheid) *a* were obtained from Wako Pure Chemical (Osaka, Japan). Protoporphyrin IX was purchased from Porphyrin Products (Logan, Utah, USA). Chls *a* and *b* were extracted from spinach leaves with acetone and were partially purified by precipitation with dioxane (Iriyama et al. 1974). The dioxane-precipitated Chls were separated and further purified by sugar-column chromatography (Perkins and Roberts 1962). Pheid *b* was prepared by acid treatment of Chl *b* according to the method of Hynninen (1973). PyroPheid *b* was prepared from Pheid *b* by dissolving Pheid *b* in pyridine and heating it in an oven at 100 ±1°C for 48 h in a sealed tube (Svec 1978). The resultant PyroPheid *b* was then identified by HPLC analysis. Mesoporphyrin IX was prepared from protoporphyrin IX by reduction with hydrogen according to the method of Shemin (1957).

Oxidation of Chls and porphyrin with chromic acid

Oxidation with chromic acid was carried out essentially as described by Rüdiger (1968, 1969). Oxidation at pH 1.2 was done at 25°C with 1% (w/v) CrO_3 solution containing 1% $KHSO_4$ for 15 min to 1 h for Chl *a* and for 1 to 15 h for Chl *b*. Oxidation of Chl *a* in 2 N H_2SO_4 was done with 1% CrO_3 in 2 N H_2SO_4 at 25°C for 1 h. In the oxidation of Chls, an equal volume of acetone was added to dissolve Chls. After the reaction, acetone was evaporated under

reduced pressure. The oxidation products were then extracted with ethyl ether and concentrated for chromatography.

Methyl esterification of the samples was carried out with a diazomethane generator (Wheaton, Millville, NJ, USA), if necessary, according to the manufacturer's instructions.

Identification of chromic acid oxidation products

The concentrated oxidation products were analyzed by thin-layer chromatography (TLC) with two solvent systems, Solvent A: dichloroethane/ethyl acetate (10:1, v/v) and Solvent B: dichloroethane/ethyl acetate/ethanol/acetic acid (200:10:5:0.5, v/v) using Kieselgel 60 plates (5 x 20 cm) (Merck, Darmstadt, Germany). Maleimides were detected by color reaction with chlorin-tetramethyl benzidine, and pyrrole aldehydes were detected with 2,4-dinitrophenylhydrazine, both basically according to the method described by Rüdiger (1969). Major bands were scraped off and extracted with ether. The ether solution was concentrated and analyzed by absorption and mass spectrometry to confirm the identification. Major compounds thus identified were separately analyzed by HPLC to determine the elution properties such as retention time. Conversely, peak fractions collected from HPLC were also analyzed with TLC under the conditions described above.

Absorption measurements were carried out with a Hitachi spectrophotometer, model U-3210 (Tokyo, Japan). Mass spectra were measured with a Hitachi mass spectrometer, M-2000AM (70 eV, Tokyo, Japan) connected with gas chromatography (GC) or liquid chromatography (LC) apparatus using an electron impact or atmospheric pressure chemical ionization methods.

HPLC

HPLC was carried out with a Shimadzu LC-10A chromatograph system (Kyoto, Japan). Separations were performed using an Asahipak ODP-50

(Showa Denko, Tokyo, Japan) (250 x 4.6 mm i.d.) packed with ODP. Degradation products were eluted with 25% (v/v) acetonitrile in water containing a final concentration of 100 mM ammonium acetate at a flow rate of 1.0 ml per min at room temperature (ca 22-25°C). Separated products were detected spectrophotometrically with a Waters LC spectrophotometer, Lambda-Max, Model 481 (Milford, MA, USA) measuring at 280 nm and quantified by a Shimadzu Chromatopac C-R6A.

Enzymatic degradation of PyroPheid a by peroxidase

PyroPheid *a* was enzymatically degraded by the action of peroxidase [EC 1.11.1.7] to ensure the applicability of this technique. The reaction was performed basically as described by Kato and Shimizu (1985). The reaction mixture contained 50 mM acetate buffer (pH 5.6), 40 μM 2,4-dichlorophenol, 8 units horseradish peroxidase (Type II) (Sigma, St. Louis, MO, USA), 20 μM PyroPheid *a* dissolved in 0.17% Triton X-100, and 15 μM H_2O_2 in a total volume of 12 ml. The reaction was started by adding H_2O_2 and measured spectrophotometrically at 665 nm. At the appropriate time periods, an aliquot was taken and degradation products were extracted with ether and the resulting ether solution was concentrated under reduced pressure to use for HPLC analyses.

Induction of senescence from plants

Seedlings of radish (*Raphanus sativus* L.) were purchased from a local market. Barley (*Hordeum vulgare* var. *hexastichon* L.) was germinated and cultivated in a growth cabinet at 25°C on wet cotton with 14-h light and 10-h dark period for 6 days. Photon fluence rate was 16.2 mmol $m^{-2} \cdot s^{-1}$. Shoots were excised and placed in 50-ml flasks containing 15 ml distilled water. The cotyledons were allowed to reach senescence in complete darkness at 25°C.

Extraction of breakdown products of Chls

Cotyledons (0.2 - 0.25 g) removed from the seedlings at various stages of senescence were ground with a small volume of cold 80% (v/v) acetone. In the case of barley, the top 1 cm was cut off and the next 6 cm from the top was used as the sample. Breakdown products of Chls were then extracted from the acetone solution with ethyl ether and concentrated under reduced pressure for HPLC analysis.

The degradation products were identified by comparison of their retention times with those obtained from authentic samples. The authentic oxidation products of PyroPheid *a* were prepared and identified chromatographically or mass spectrometrically as described previously (Suzuki et al. 1999).

Chl contents

The Chl content of senescent leaves was determined in 80% (v/v) acetone extract using the absorption coefficients of Mackinney (1941). The absorption measurements were performed with a Hitachi spectrophotometer, model U-3210 (Tokyo, Japan), at room temperature.

Results

Identification of authentic oxidation products

Oxidation of mesoporphyrin IX with chromic acid is known to yield two monopyrroles, HA and MEM (Shemin 1957). These two compounds were separated by TLC and identified as described in the Experimental section. The ratio of front (R_f) values obtained from TLC using solvent B were 0.16 for HA and 0.61 for MEM. The molecular masses of these compounds were determined by mass (MS) analyses: 139 (M^+) for MEM by GC- MS with electron impact method; 183 (M^+) for HA by LC-MS with atmospheric pressure chemical ionization method.

Oxidation products of PyroPheid *a* with chromic acid gave additional

components, methyl vinyl maleimide (MVM) and C-E-ring derivative of Chl in addition to the above two compounds, as demonstrated by Shimomura (1980). These compounds were clearly separated by TLC in a solvent system with B, and the R_f values of MVM and C-E-ring derivative were 0.64 and 0.28, respectively. Besides these compounds, one more aldehyde compound (R_f = 0.63 in solvent B) was detected by color reaction with dinitrophenylhydrazine as described by Shimomura (1980). This compound was tentatively identified as degraded C-E-ring derivative from the presence of aldehyde. The appearance of this peak in oxidation products from Chl *a* and in enzymatic degradation will be described below.

Separations of degradation products

The effect of acetonitrile concentration in the presence of 100 mM ammonium acetate on the logarithm of the capacity factors, *k'*, a measure of retention of monopyrroles and C-E-ring derivative is shown in Fig. V-2. The values of the logarithm of the capacity factors of four oxidation products increased with decreasing acetonitrile concentration and the individual plots gave parallel lines. This indicates that the ratio of the capacity factor, α, is not changed with increasing mobile phase polarity. It means further that the order of elution of degradation products is constant independent of polarity. Omission of ammonium acetate resulted in the slight decrease of peak resolution due to weak retention of ionic compounds. This largely varied depending on the ODS column used. The elution order of the compounds remained unchanged in a presence or absence of ammonium acetate.

The separation of esterified and non-esterified samples in the presence of ammonium acetate was compared. There were, however, no significant differences between their separation parameters such as capacity factors and resolution. The separation of MEM and MVM can be reproducibly performed using an ODP column, but not the usual ODS column (see below and Fig. V-4). Thus, the use of an ODP column with 25% acetonitrile in water containing a

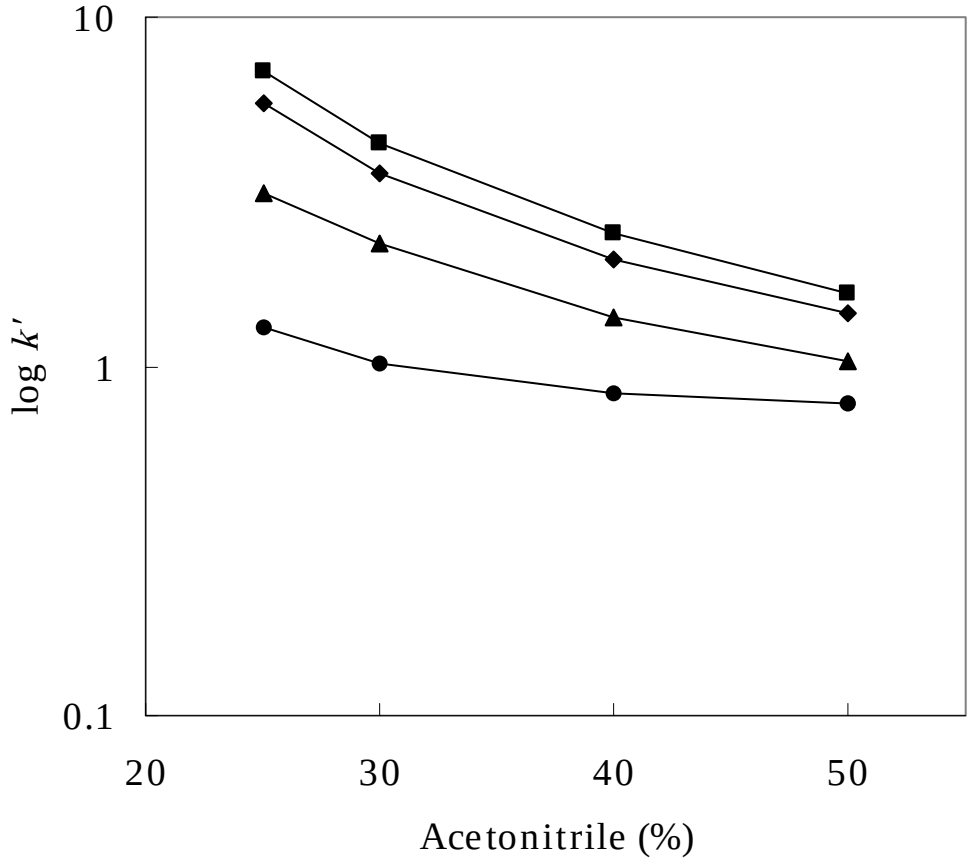

Fig. V-2. Acetonitrile concentration dependency on the logarithm of the capacity factor (k') of the separatedoxidation products. The isolated oxidation products were eluted with the indicated percentage of acetonitrile in water containing 100 mM ammonium acetate. The separation was carried out with an ODP column at a flow rate of 1.0 ml per min at room temperature. The oxidation products were measured spectrophotometrically at 280 nm. The capacity factors of the separated compounds were calculated as in Table 1. ●, hematinic acid; ▲, C-E-ring derivative; ◆, methyl ethyl maleimide; ■, methyl vinyl maleimide.

final concentration of 100 mM ammonium acetate is suitable for the separation of oxidation products, in particular monopyrrole derivatives of Chls and porphyrins.

The repeatability of the separation in this system strongly depends on several factors. The coefficient of variation of the retention times approached 2.8% as calculated from 13 measurements of MEM at ambient temperature. This slightly poor repeatability is due mainly to the fact that the retention strongly depends on the mobile phase polarity, as can be seen in Fig. V-2, and also column temperature which changes the viscosity of the eluent. To attain good repeatability of the retention times for identification, a fixed column temperature is recommended. The retention times, the values of the capacity factor, k', and α values of oxidation products of PyroPheid *a* are presented in Table V-1.

Fig. V-3 shows the separation of extracts of oxidation products of mesoporphyrin IX under the suitable elution conditions noted above. The oxidation products were separated in less than 12 min. Peak 1 with a retention time at 2.9 min was HA and peak 2 with a retention time at 10.1 min was MEM by the comparison with authentic samples. A peak at 2.4 min and peaks that appeared around 6 to 7 min were unknown degradation products. Peaks emerged that around 17 to 19 min are not determined yet, but are probably dipyrrole derivatives from comparison with photodegradation products of bilirubin. The presence of dipyrrole derivatives in the oxidation products was supported by mass analysis.

The extract of oxidation products of PyroPheid *a* was analyzed on an ODP column with a 25% acetonitrile in water containing 100 mM ammonium acetate (Fig. V-4). The oxidation products were separated in less than 14 min. Peak 1 with a retention time at 2.9 min was HA and peak 2 at 6.5 min was determined to be C-E-ring derivative of Chl by comparison with authentic samples. Peaks 3 (t_R = 10.1 min) and 4 (t_R = 12.1 min) were MEM and MVM, respectively. The structure of these compounds is very similar, and

Table V-1. Separation of chemical oxidation products of mesoporphyrin IX and pyropheophorbide *a* by HPLC using an ODP column

Oxidation product	t_R (min)	k'	α
Hematinic acid	2.93	0.768	1.00
C-E-ring derivative	6.52	2.93	3.81
Methyl ethyl maleimide	10.13	5.10	6.64
Methyl vinyl maleimide	12.10	6.29	8.20

The oxidation products were eluted with 25% acetonitrile in water containing 100 mM ammonium acetate at a flow rate of 1.0 ml per min at room temperature. Other chromatographic conditions as in the text. Retention times, t_R, were read directly from a Chromatopac C-R6A and expressed as the mean values from three to five experiments. The capacity factor, k', is given by $k' = (t_R - t_0)/t_0$, where t_R and t_0 are the retention times of retained and unretained solutes, respectively. The ratio of capacity factors, α, is calculated by $k'/k'_{\text{heamtinic acid}}$.

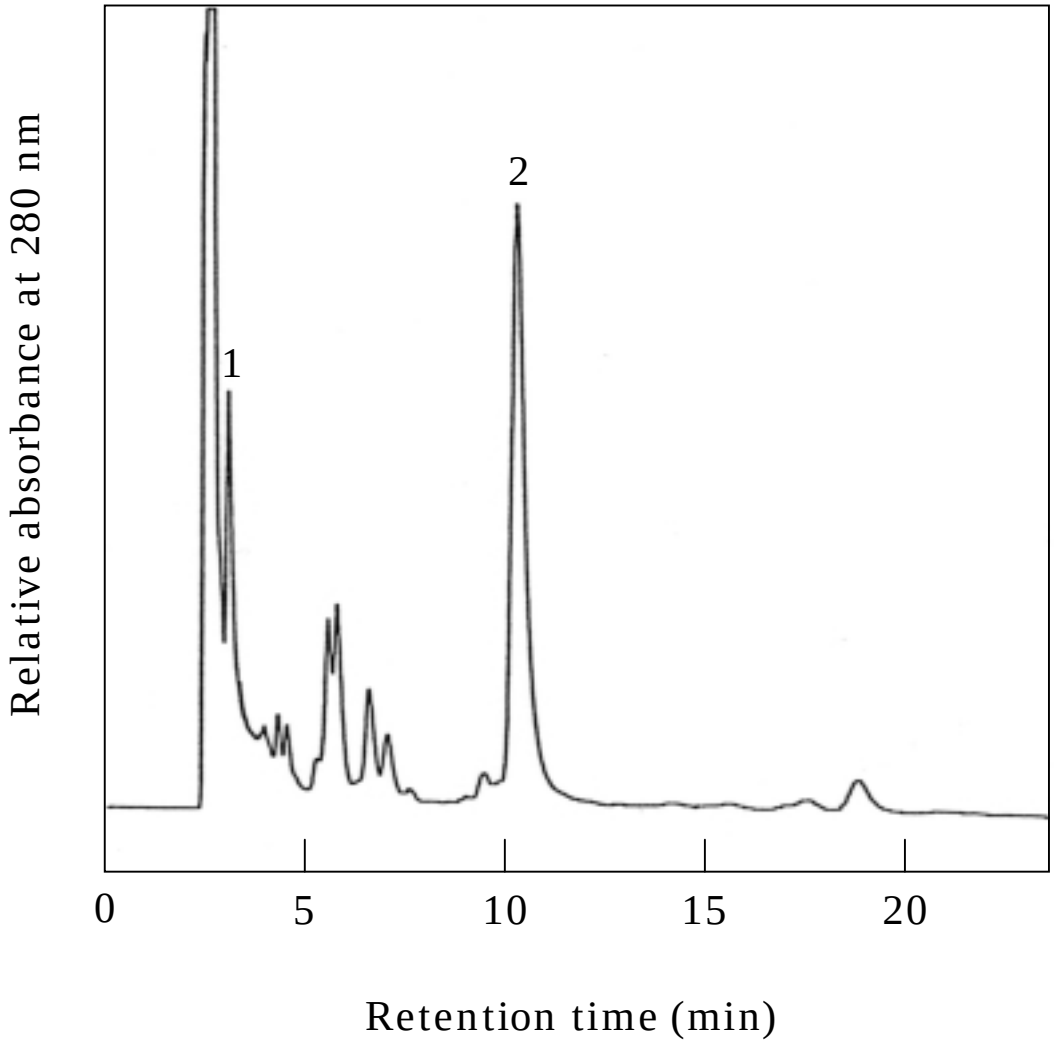

Fig. V-3. HPLC elution profile of extract of chemical oxidation products of mesoporphyrin IX with chromic acid. Chemical oxidation and extraction of the products are described in the text. The oxidation products were eluted with 25% acetonitrile in water containing 100 mM ammonium acetate. Other chromatographic conditions and detection methods as in Fig. V-2. Peaks: 1, hematinic acid; 2, methyl ethyl maleimide; Non-numbered, unknown degradation products.

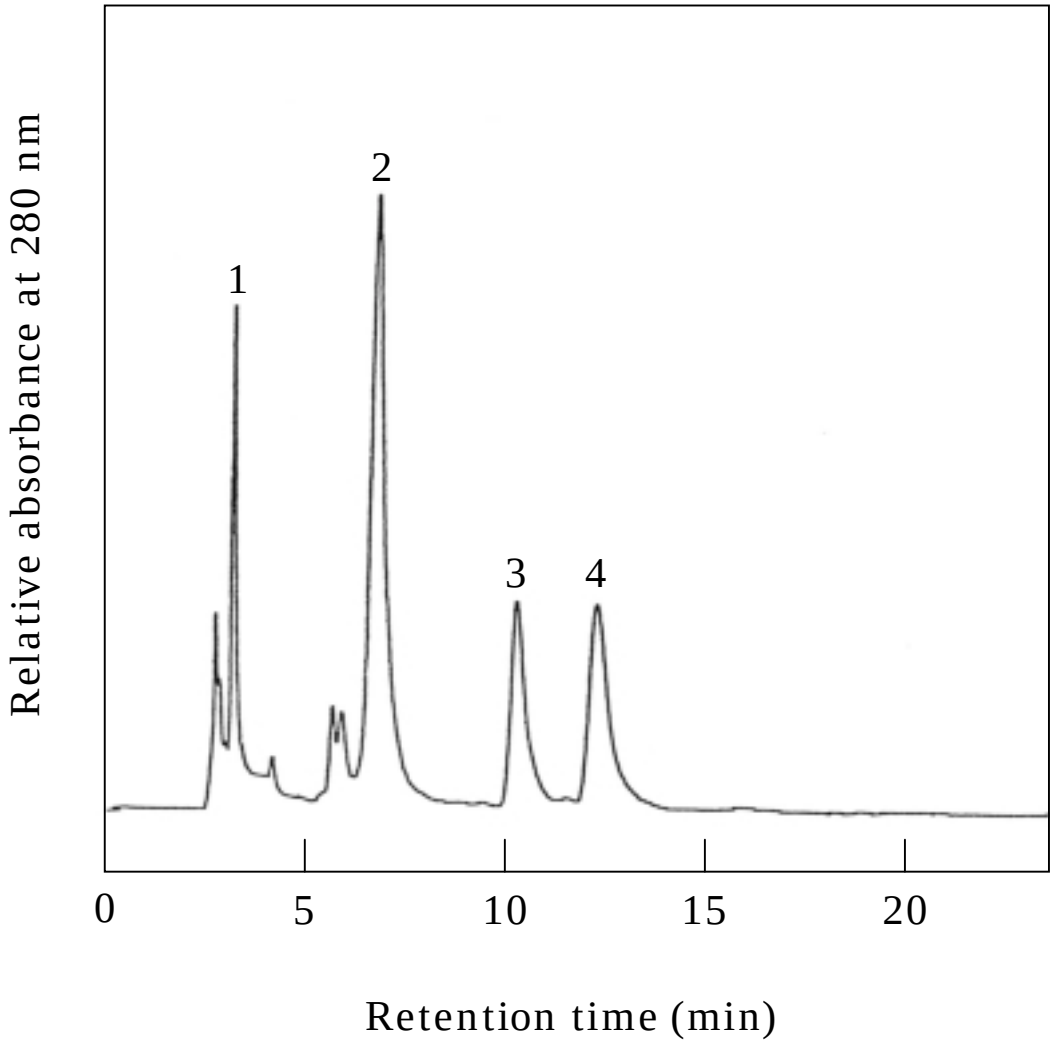

Fig. V-4. HPLC elution profile of extract of chemical oxidation products of pyropheophorbide *a* with chromic acid. Chemical oxidation and extraction of the products are described in the text. HPLC conditions as in Fig. V-3. Peaks: 1, hematinic acid; 2, C-E-ring derivative; 3, methyl ethyl maleimide; 4, methyl vinyl maleimide; Non-numbered, unknown degradation products.

differentiation could not be resolved completely by the usual ODS column (Shioi et al. 1995). However, the ODP column that was used here was capable of the separation of these ethyl and vinyl species as reported previously (Shioi et al. 1995).

In the case of oxidation in more acid conditions, a new peak appeared between peaks 4 (MEM) and 5 (MVM). This peak was tentatively identified as degraded C-E-ring derivative from TLC analyses. This compound is found commonly in the enzymatic degradation products (see Fig. V-5A, peak 2) and in the senescent cotyledons of higher plants (Suzuki and Shioi 1999).

Faint peaks eluted around 17 to 19 min were also found in this extract of short-term oxidation with chromic acid and these are tentatively identified as dipyrrole derivatives as described above. Peaks that appeared at 2.4 min and around 6 to 7 min were unknown degradation products. Interestingly, these degradation products can be seen in the extracts obtained from both mesoporphyrin IX and PyroPheid *a*. It is likely that these may be derived by further degradation of main compounds and they appear to have a similar structure from their elution properties.

With respect to the separation of PyroPheid *b*, HA and C-E-ring derivative were clearly separated. Two other primary products, methyl vinyl and methyl formyl maleimides were eluted as a mixture with similar retention times as MEM and MVM. However, their identities could not be resolved completely with the samples that had been prepared with oxidation times from 1 to 15 h.

Application

The present method was applied to analyze oxidation products of PyroPheid *a* by the enzymatic reaction with peroxidase. This experiment was constructed as a model of Chl degradation by biological system using a simple enzymatic reaction. As shown in Fig. V-5A, four peaks and one shoulder were clearly observed. These were compared to the standard sample to identify

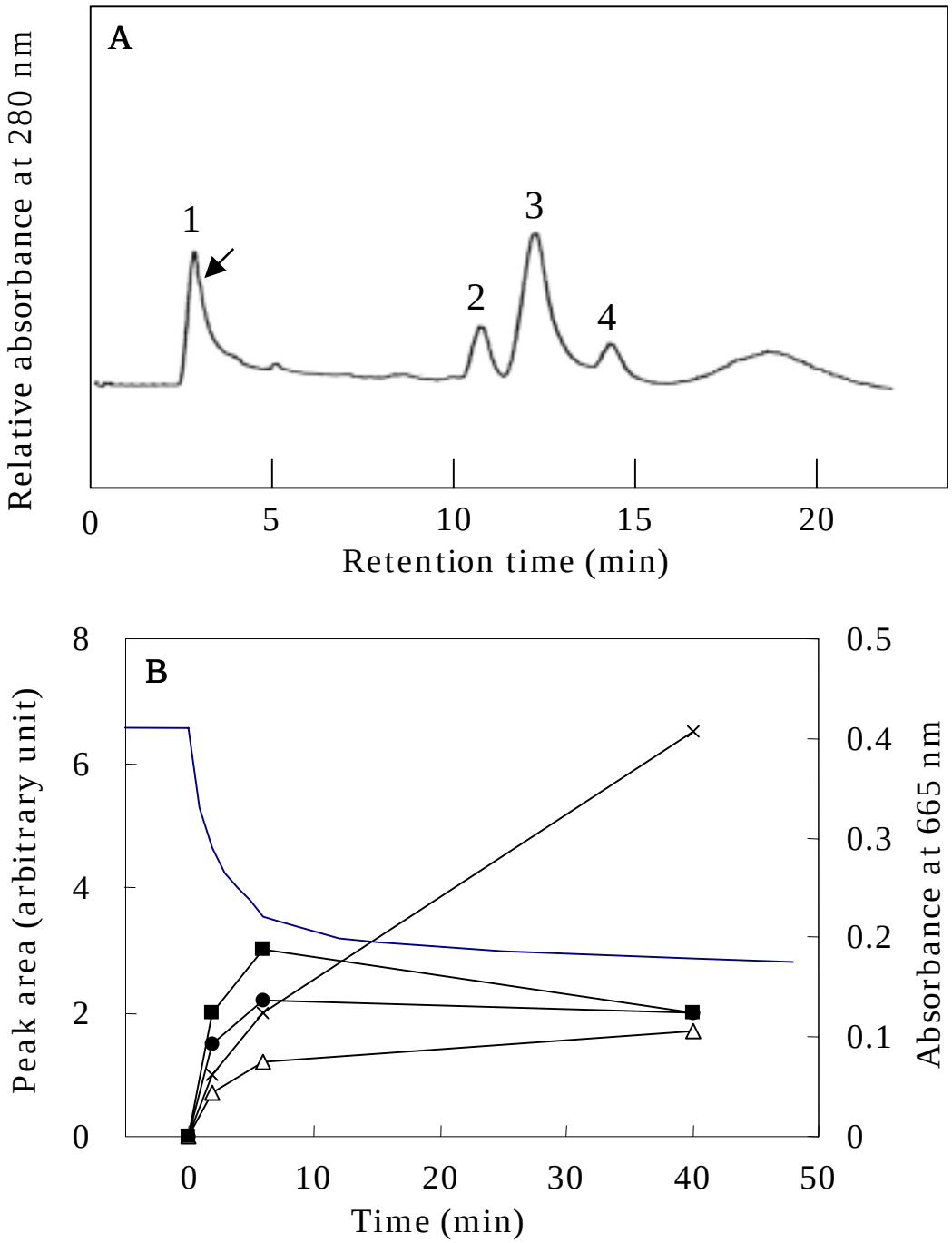

Fig. V-5. (A) HPLC elution profile of extract of enzymatic degradation products of pyropheophorbide *a* by peroxidase reaction. Enzymatic degradation and extraction of the products are described in the text. HPLC conditions as in Fig. V-3. Peaks: 1, unknown compounds; 2, degraded C-E-ring derivative; 3, methyl vinyl maleimide; 4, 2,4-dichlorophenol; shoulder (arrow), hematinic acid. Non-numbered peaks were no identified. (B) Time-dependent change of degradation products in enzymatically degraded pyropheophorbide *a*. Contents of oxidation products were estimated by HPLC as described in (A). Content of pyropheophorbide *a* was determined spectrophotpmetrically measuring at 665 nm. ×, unknown product(s); ●, hematinic acid; △, degraded C-E-ring derivative; ■, methyl vinyl maleimide. Solid line without symbol, pyropheophorbide *a* (right scale)

peak compounds. Peak 1 was hydrophilic compounds probably derived from further degradation of pyrrole derivatives. The shoulder around 2.9 min contained HA. Peak 2 (t_R = 11.2 min) was tentatively identified as degraded C-E-ring derivative as described above. Peak 3 (t_R = 12.1 min) is assigned as MVM from the comparison of the standard sample. Peak 4, which appeared at around 15 min, was 2,4-dichlorophenol used as a cofactor for the enzymatic reaction, from coelution and the comparison with an authentic sample.

The time course of formation of enzymatic breakdown products of PyroPheid *a* is shown as well as the decrease of PyroPheid *a* (Fig. V-5B). Three degradation products, HA, MVM, and degraded C-E-ring derivative increased sharply up to 5 min with a concomitant decrease of PyroPheid *a*. Unknown hydrophilic compound(s), which appeared with a slight lag time from the first three compounds, may be due to further degradation of main monopyrroles into more hydrophilic low molecular mass compounds, although further quantitative study is necessary to obtain the stoichiometric answer. Similar to the photodegradation of bilirubin (Lightner 1977), degradation of PyroPheid *a* through enzymatic reaction is first initiated by a break of the bridge linkage and subsequent hydrolytic reactions leading to the formation of hydrophilic compounds such as simple organic acids.

Chl breakdown during senescence in higher plants

Chl contents in the senescent cotyledons of barley and radish were followed spectrophotometrically after extraction of Chls (Fig. V-6). Chl content was slightly higher in the cotyledons of radish than barley on a fresh weight basis and the Chl *a* to *b* ratio in both plants was nearly the same, at about 2.8, before senescence. Chl content in both plants was gradually decreased with increasing day of senescence and reached 32.4% for radish and 26.4% for barley after 5 days. The Chl *a* to *b* ratio decrease was almost parallel with the Chl decrease in senescent cotyledons of radish. In barley, however, Chl *b* decrease was somewhat slower than Chl *a*, and the Chl *a* to *b* ratio reached 2.2 at 5 days

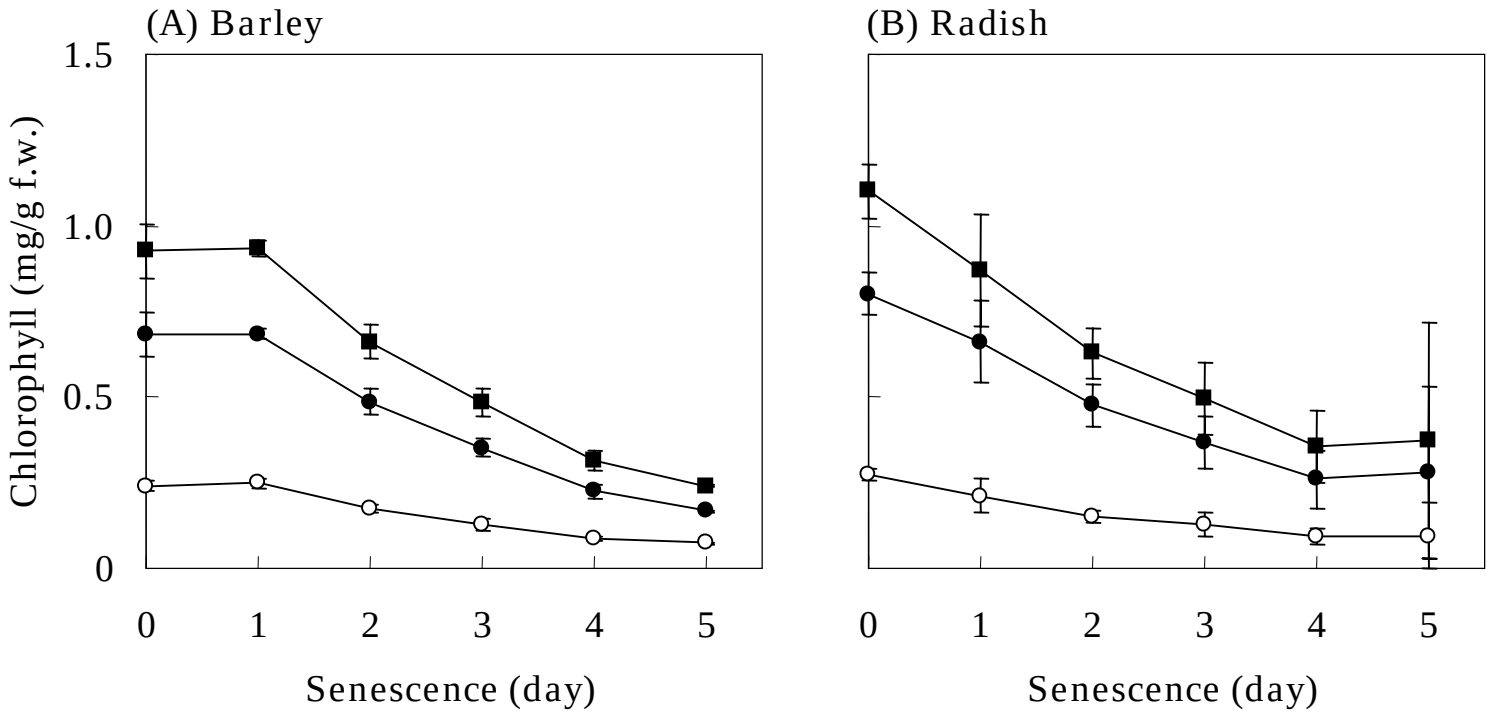

Fig. V-6. Degradation of chlorophylls during senescence. Chls were extracted with 80% (v/v) acetone from cotyledons of the indicated day of senescene and measured spectrophotometrically. Vertical bar indicates the standard deviation calculated from 3 to 5 independent experiments. ■, Total Chls; ●, Chl *a*; ○, Chl *b*.

of senescence.

Determination of breakdown products of Chls from barley

Fig. V-7 shows the HPLC separation profile of extracts of breakdown products of Chls during senescence of barley on an ODP column eluted with 25% (v/v) acetonitrile-water containing 100 mM ammonium acetate (also see Table V-2). The breakdown products were separated in less than 12 min. Peak 2 (retention time, t_R = 2.9 min) was HA, and peak 0 (t_R = 2.4 min), which appeared around t_0, was unknown product(s). Peaks 3 and 4 appear not to be Chl degradation products from their retention times and absorption peaks. Peak 5 (t_R = 10.1 min) was MEM by comparison with the authentic sample. MVM and C-E-ring derivative of Chl, which have been found in the chemical oxidation products of Chls, were not detected in the barley. Instead, a new peak 6 (t_R = 11.2 min) emerged and was tentatively identified as degraded C-E-ring derivative, a putative MVM dialdehyde from its elution properties (Suzuki et al. 1999). The absence of MVM suggests that it may be rapidly metabolized during senescence. Methyl formyl maleimide, a degradation product of Chl *b*, was not detected in this experiment (see Discussion).

The time course of formation of breakdown products of Chls in senescent cotyledons of barley is presented in Fig. V-8. Except for a peak, which appeared around t_0 and a small amount of HA, degradation products of Chls were negligible both in pre- and one-day senescent cotyledons. This finding is consistent with the lack of Chl loss at one day in senescent cotyledons (Fig. V-6). MEM and degraded C-E-ring derivative both reached maximum at 2-day senescence. MEM decreased gradually but kept a high level during senescence, while degraded C-E-ring derivative decreased during senescence and reached almost zero at 5-day senescence. HA increased only slightly during senescence.

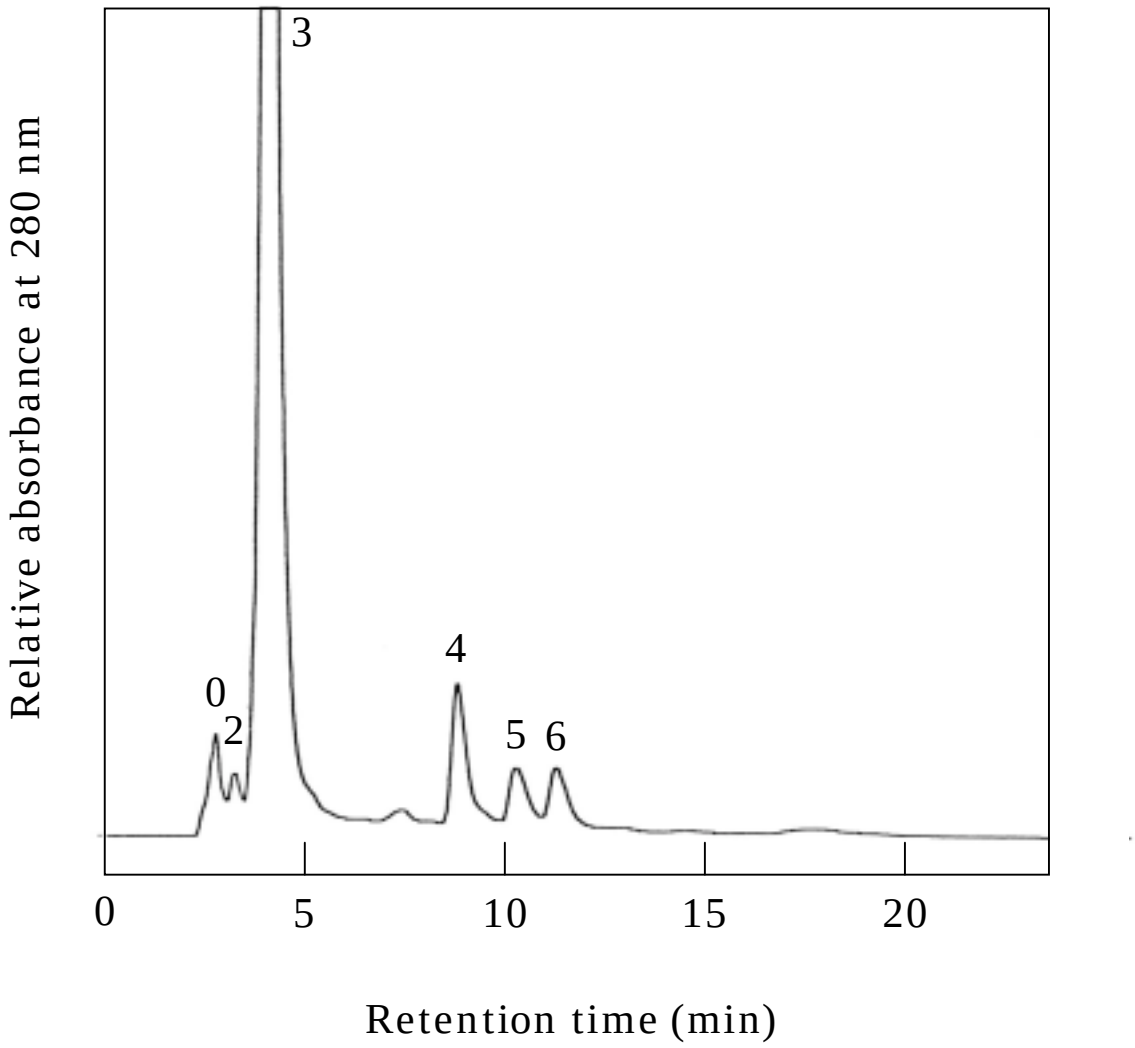

Fig. V-7. HPLC elution profile of extract of senescent cotyledons of barley. The degradation products were extracted from 4-day senescent cotyledons. Procedures of senescence and extraction of the products are described in the text. HPLC conditions as in Fig. V-3. Peaks: 0, unknown compounds; 2, hematinic acid; 3 and 4, unknown; 5, methyl ethyl maleimide; 6, degraded C-E-ring derivative.

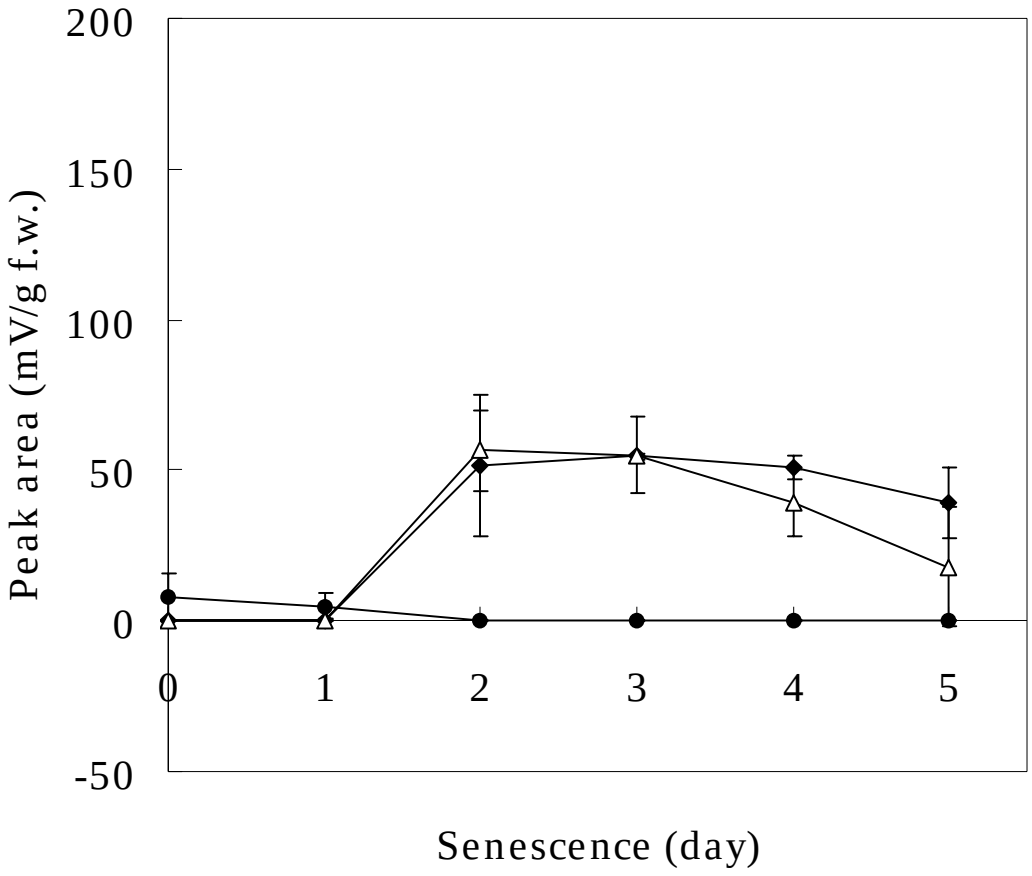

Fig. V-8. Time-dependent change of degradation products in senescent cotyledons of barley. Concentrations of oxidation products estimated by HPLC on the indicated days of senescent cotyledons, as described in Fig. V-7, were plotted. Vertical bar indicates the standard deviation calculated from 3 to 5 independent experiments. ●, hematinic acid; ◆, methyl ethyl maleimide; △, degraded C-E-ring derivative.

Determination of breakdown products of Chls from radish

The extract of breakdown products of Chls during senescence of radish cotyledons was separated by HPLC in a similar manner (Fig. V-9 and Table V-2). The HPLC profile shows that the separation of breakdown products was completed in less than 14 min. Peak 2 (t_R = 2.9 min) was HA, and peaks 5 (t_R = 10.1 min) and 7 (t_R = 12.3 min) were MEM and MVM, respectively, by comparison with authentic samples. The structure of these maleimides is very similar, and they cannot be differentiated completely by the usual ODS column. However, the ODP column that was used here enables the separation of these molecular species as described previously (Shioi et al. 1995; Suzuki et al. 1999). Similar to the results for barley, peak 0 that appeared around t_0 and peak 6 (t_R = 11.2 min) of degraded C-E-ring derivative, were found, but C-E-ring derivative itself was not detected. Peaks 1 (t_R = 2.7 min) and 3 were unknown degradation products, but peak 1 was characteristic in senescent cotyledons of radish. Methyl formyl maleimide, a degradation product of Chl *b*, was not detected, as in the case of barley (see Discussion).

Fig. V-10 shows the time course of formation of breakdown products of Chls in senescent cotyledons of radish. The main monopyrrole derivatives of Chl degradation products including degraded C-E-ring derivative were detected in radish. Surprisingly, the concentrations of these main monopyrrole derivatives were highest in pre-senescent cotyledons and decreased during senescence, although they displayed different time courses. This phenomenon is characteristic of radish cotyledons (see Discussion) and can be observed regardless of senescence with freshly harvested 6- to 7-day greening cotyledons. Increases at 3-day senescence in HA (peak 2) and a hydrophilic compound eluted at 2.7 min (peak 1)(data not shown) may reflect the additional increase in degradation products derived from Chl loss during senescence (see Fig. V-6 and Discussion).

Main degradation products of Chls detected in senescent cotyledons of higher plants and enzymatic oxidation products of PyroPheid *a* are summarized

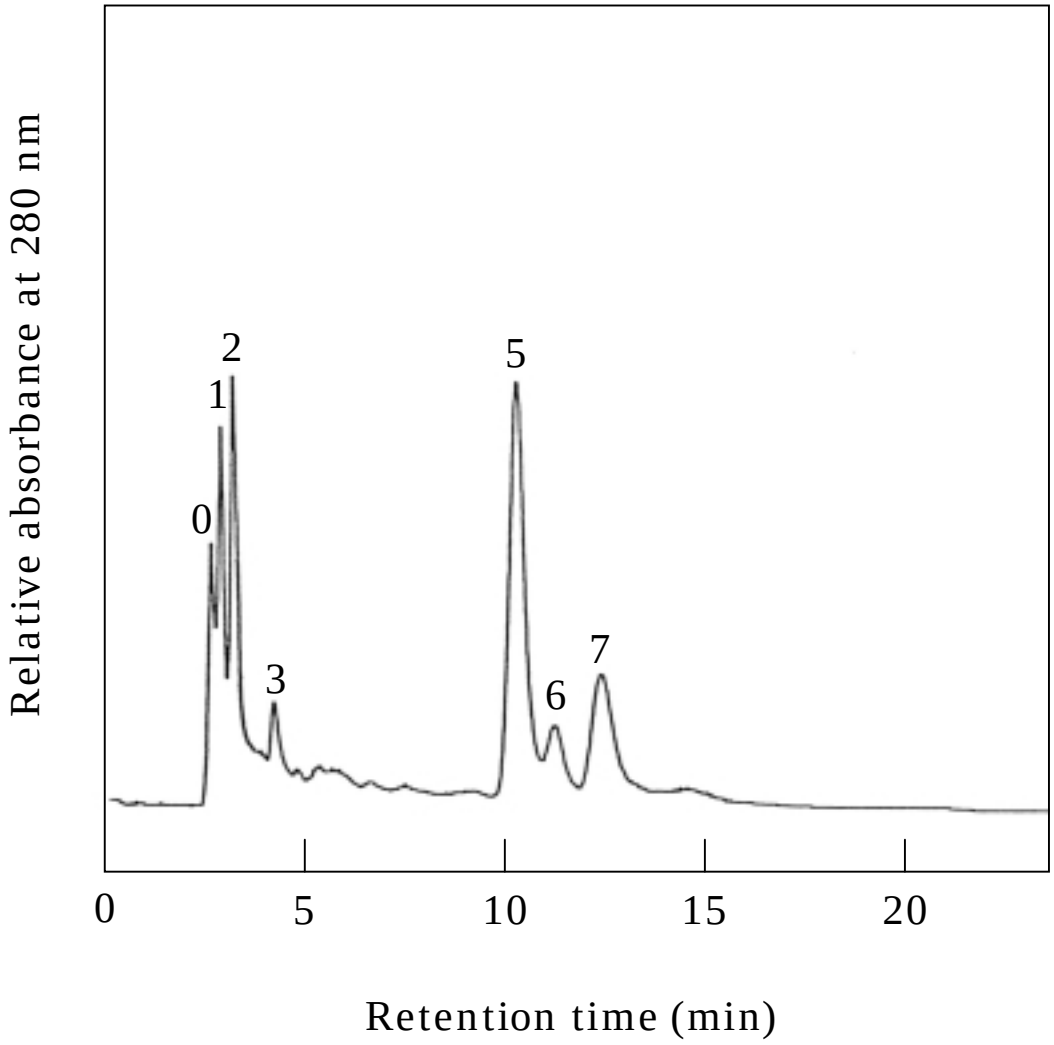

Fig. V-9. HPLC elution profile of extract of senescent cotyledons of radish. The degradation products were extracted from 4-day senescent cotyledons. Procedures of senescence and extraction of the products are described in the text. The separation and detection of products were done as described in Fig. V-3. Peaks: 0 and 1, unknown compounds; 2, hematinic acid; 3, unknown; 5, methyl ethyl maleimide; 6, degraded C-E-ring derivative; 7, methyl vinyl maleimide .

Table V-2. Degradation products of chlorophylls in senescent cotyledons of higher plants and enzymatic oxidation of pyropheophorbide *a*

Peak[a]	t_R (min)	Barley	Radish	PyroPheid *a*[b]	Identification
1	2.7	−	+	−	N.D.[c]
2	2.9	+	+	+	Hematinic acid
	6.5	−	−	−	C-E-ring derivative
5	10.1	+	+	−	Methyl ethyl maleimide
6	11.2	+	+	+	Putative degraded C-E-ring derivative
7	12.3	−	+	+	Methyl vinyl maleimide

[a]Corresponding to the peak numbers in Fig. V-7 and V-9.

[b]Cited from Suzuki et al. (1999).

[c]Not determined.

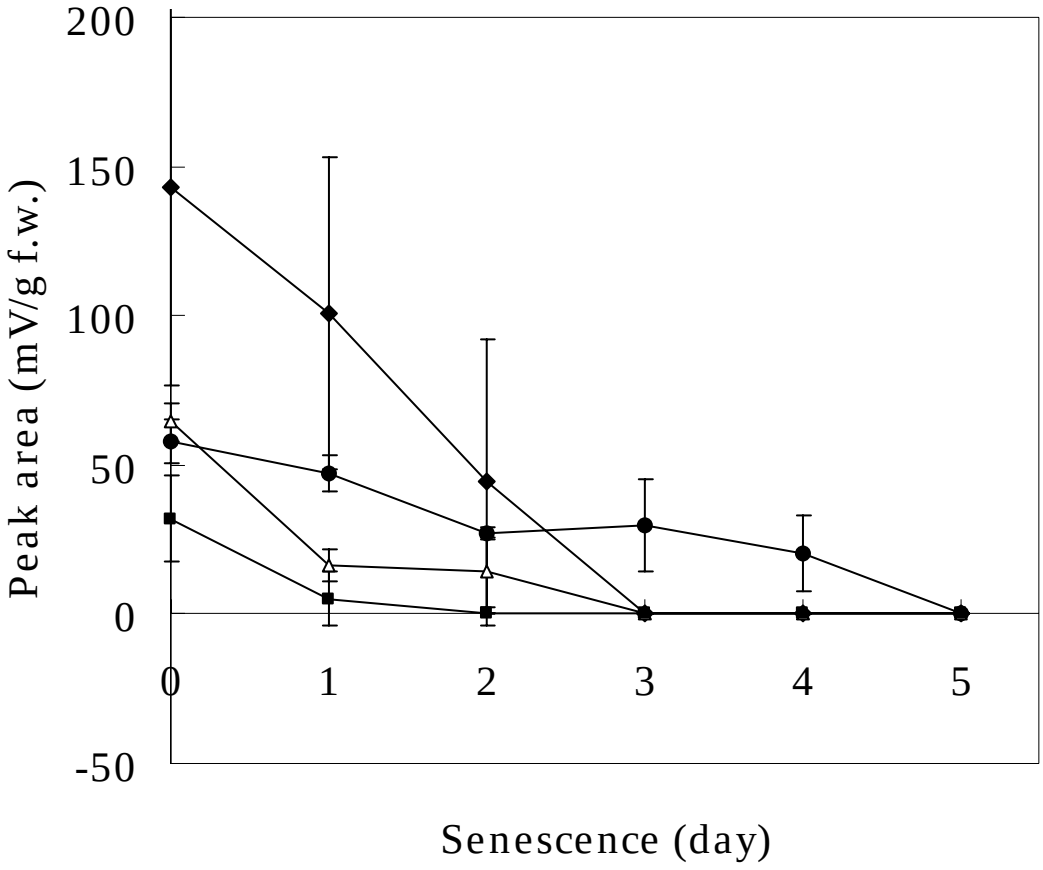

Fig. V-10. Time-dependent change of degradation products in senescent cotyledons of radish. Contents of oxidation products estimated by HPLC in the indicated days of senescent cotyledons, as described in Fig. V-9, were plotted. Vertical bar indicates the standard deviation calculated from 3 to 5 independent experiments. ●, hematinic acid; ◆, methyl ethyl maleimide; △, degraded C-E-ring derivative; ■, methyl vinyl maleimide.

in Table V-2. Interestingly, HA and degraded C-E-ring derivative are commonly found in barley, radish and enzymatically oxidized PyroPheid *a* (Suzuki et al. 1999). However, C-E-ring derivative itself was not detected in any of the samples tested.

Discussion

The results presented here show that degradation products of Chls were clearly detected in senescent cotyledons of barley and in both pre- and senescent cotyledons of radish. These include HA, MEM, MVM, degraded C-E-ring derivative, and also their hydrophilic degradation product(s). C-E-ring derivative, which is usually formed in the chemical oxidation of Chls with chromic acid, was, however, not detected in these plant species nor was enzymatic degradation by peroxidase (Suzuki et al. 1999) (Table V-2). This is probably due to the weakness of the isocyclic ring, which is attacked by several chemical modifications, including oxidation, leading to breakdown of the ring structure (Seely 1966). At present, we could not determine the stoichiometric relation between amounts of Chl degraded and the sum of formed degradation products because of the difficulty of purification and determination of concentration of each product.

Besides barley, the degradation products of Chls were detected only in the senescent leaves and cotyledons in several higher plants that had lost Chls, including spinach, pea and komatsuna (rape group) leaves and cucumber cotyledons. As shown in barley, senescence caused yellowing, and the rate of Chl decrease likely correlated with the appearance of degradation products. Exceptionally, in the case of radish, degradation products were found even in the pre-senescent cotyledons that lack apparent Chl loss. Degradation products that emerged after 2-day senescence would include the products corresponding to the real Chl loss during senescence as can be seen by a relative increase at a later stage of senescence (see Figs. V-6 and V-8). This is

in accordance with the finding that decay of bilin derivative, a precursor of pyrroles, occurs after 2 days of senescence (Watanabe, M. in preparation). This result raises the question of where these first products came from? At present we have no exact answer to this question, but it might happen if turnover of Chls is fast and synthesis and breakdown of Chls is balanced before senescence in cotyledons of radish, as described by Walmsley and Adamson (1994).

The hydrophilic compound(s) eluted at 2.7 min is characteristic in radish and seems to be accumulated with a concomitant decrease of the main monopyrrole derivatives. This may be hydrophilic low-molecular-mass-degradation product(s) of monopyrroles, although further stoichiometric study is needed. The appearance of hydrophilic compound(s) is clearly supported by a previous study that was constructed as a model of Chl degradation by biological systems using a simple enzymatic reaction with peroxidase (Suzuki et al. 1999). In that experiment, compounds eluted around 2.4 min were studied and found to be derived from degraded pyrrole derivatives of a hydrophilic nature. Since the system contained solely PyroPheid *a*, no products other than the pigment can be considered. Furthermore, the rate of appearance of the hydrophilic compounds clearly correlated with the decrease of the main monopyrroles. These results suggest that monopyrrole derivatives are fated to degrade further into simpler hydrolytic products, as can be seen in photodegradation products of Chl (Llewellyn et al. 1990a, 1990b) and bilirubin (Lightner 1977).

In this study, the putative methyl formyl maleimide that is derived only from the degradation products of Chl *b* could not be detected, although Chl *b* has a low susceptibility to chemical oxidation with chromic acid and could not be completely separated by HPLC (Suzuki et al. 1999). This finding is consistent with the report of Hörtensteiner et al. (1995) that Chl *b* could not serve as the substrate for Pheid *a* oxygenase, a ring-opening enzyme (see Fig. I-1). This means that Chl *b* itself is not degraded, but Chl *b* can break down

after conversion to Chl *a*, as has been reported by Ito et al. (1993).

Accumulation of the main monopyrrole derivatives including hydrophilic compound(s) is obvious in the degradation of Chls in this and previous studies (Suzuki et al. 1999). Further, C-E-ring derivative itself and degradation products of Chl *b* were not detected in the samples tested (see Table V-2). These facts suggest that a common pathway leading to the formation of definite products may be present in the degradation of Chls, although the mode of degradation of Chls is largely different between plant species. As demonstrated in the previous study (Suzuki et al. 1999), formation of monopyrroles from Chl by enzymatic reaction other than non-enzymatic photooxidation is possible (Jen and Mackinney 1970; Llewellyn et al. 1990a, 1990b). This is supported by the fact that monopyrroles were produced in the senescent leaves under total darkness without involvement of photooxidation. However, we have, as yet, no information on the enzymatic formation of the compounds during breakdown of Chl in vivo.

Similar to the photodegradation of bilirubin (Lightner 1977), degradation of bilin derivatives in higher plants is first initiated by a break of the bridge linkage leading to the formation of monopyrrole derivatives probably via dipyrrole derivatives. Subsequently, the monopyrroles formed are degraded further by successive hydrolytic reactions to hydrolytic monopyrroles and finally to organic acids, as described in the products of photodegradation of Chls (Llewellyn et al. 1990a, 1990b). These organic acids may be used as nutrients for plants by virtue of sink-source relation.

Chapter VI

Conclusion

In this thesis, the author presented new findings from the results of four main studies on the chlorophyll (Chl) degradation, as described in detail in Chapters II to V. In this Chapter VI, the results of the studies are discuss and conclude in relation to the present understanding of Chl breakdown in intact plants, especially, some approaches toward the localization of breakdown of Chls.

Based on the combined data demonstrated in this study, the author would like to propose the idea of the presence of extraplastidic and multiple degradation pathways in the breakdown of Chls. A tentative compartmentation of the degradation pathway of Chl is shown in Fig. VI-1. The chlorophyllase (Chlase) reaction is the first step in Chl degradation. Two Chlase homologues are isolated in *Arabidopsis thaliana*. One has a typical transit peptide for import to the chloroplasts, whereas the other does not have typical peptide. The Chlase of *Chenopodum album* contains a signal peptide for the endoplasmic reticlum (Tsuchiya et al. 1999). It is not doubt from these facts that one of the Chlase isozymes is located in plastids. Furthermore, in the final step of the early stage, the enzymes acted in the formation of pyropheophorbide (PyroPheid) are induced during senescence and are located in cytosol. And pheophorbidase, which catalyze the reaction of PyroPheid formation, did not have transit peptide (see in Chapter IV, Discussion). These results obviously indicate that Chl degradation occurs in the extraplastic conditions (Suzuki and Shioi 2001, Suzuki et al. 2002). If these enzymes exist in an organelle other than the chloroplasts, one important question rises for us, how Chl molecules transport from the thylakoids to these enzymes and degradation proceeds. One of candidates for the carrier of Chl is the plastoglobuli. There are several reports supporting this fact that numerous large plastoglobuli containing Chls and Chl-protein complexes were extruded into the cytosol through the senescent chloroplast envelope membrane (Guiamét et al. 1999 and references therein). In addition, connections or fusions between plastid and virtually every other organelle have previously

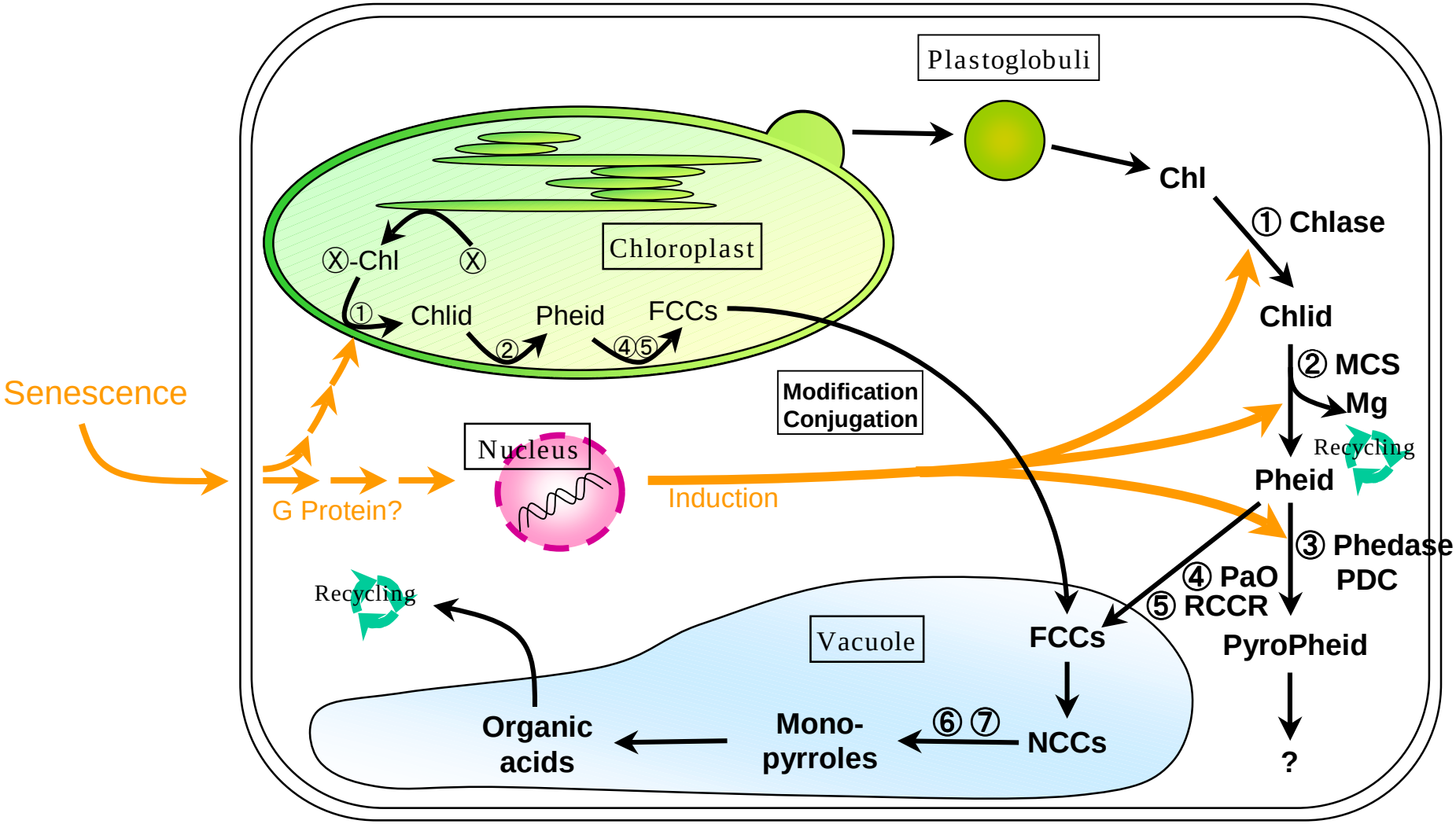

Fig. VI-1. Hypothetical pathway of Chl degradation in inside and outside of chloroplasts. An unknown factor (X) is responsible for the removal of Chl from the thylakoid. Question mark denotes unknown reaction. The numbers are corresponding to Fig. I-1. Abbreviations: Chl, chlorophyll; Chlid, chlorophyllide; Pheid, pheophorbide; PyroPheid, pyropheophorbide; FCCs, fluorescent Chl catabolites; NCCs, nonfluoresent Chl catabolites.

been reported (Crotty and Ledbetter 1973; Wellburn and Wellburn 1979). These connections could allow for transfer of material from organelle to organelle. Endoplasmic reticula have been shown to be connected to the plastid envelope (Crotty and Ledbetter 1973; Ekes 1979). Another route from plastid to vacuole was suggested by the study of Vaughn and Duke (1981). They suggested that vacuoles were formed from plastid evaginations and this might allow for transfer of material in the plastid to vacuole. As a result, the author concluded that Chl degradation might not be limited to the inside of chloroplasts.

As shown in Fig. VI-1, Chls are degraded successively in outside of chloroplasts, probably in vacuoles by cleavage of macrocyclic ring and subsequent hydrolytic reactions via monopyrroles to finally organic acids. The formed organic acids may be recycled as nutrients for plant by sink-source mechanism (Suzuki et al. 1999, Suzuki and Shioi 1999).

Finally, our idea, the presence of the extraplastidic pathway of Chl degradation, might lead to a new insight into elucidating the catabolic mechanism of the components in the chloroplasts.

References

Altschul, S. F., Madden, T. L., Schäffer, A. A., Zhang, Z., Miller, W. and Lipman, D. J. (1997) Gapped BLAST and PSI-BLAST: a new generation of protein database search programs. *Nucl. Acids Res.* 25: 3389-3402.

Azuma, R., Takahashi, Y., Kurata, H., Kawano, T., Shimokawa, K. and Adachi, M. (1999) Does peroxidase act as a 'Mg-dechelatase'? *Plant Peroxidase Newslett.* 13: 145-151.

Benedetti, C. E., Costa, C. L., Turcinelli, S. R. and Arruda, P. (1998) Differential expression of a novel gene in response to coronatine, methyl jasmonate, and wounding in the *Coi1* mutant of Arabidopsis. *Plant Physiol.* 116: 1037-1042.

Benedetti, C. E. and Arruda, P. (2002) Altering the expression of the chlorophyllase gene *ATHCOR1* in transgenic Arabidopsis caused changes in the chlorophyll-to-chlorophyllide ratio. *Plant Physiol.* 128: 1255-1263.

Bennett, M. J., Choe, S. and Eisenberg, D. (1994) Domain swapping: Entangling alliances between proteins. *Proc. Natl. Acad. Sci. USA* 91: 3127-3131.

Biswal, B., Choudhury, N. K., Sahu, P. and Biswal, U. C. (1983) Senescence of detached fern leaves. *Plant Cell Physiol.* 24: 1203-1208.

Biswal, B., Rogers, L. J., Smith, A. J. and Thomas, H. (1994) Carotenoid composition and its relationship to chlorophyll and D1 protein during leaf development in a normally senescing cultivar and a *stay-green* mutant of *Festuca pratensis*. *Phytochemistry* 37: 1257-1262.

Biswal, B. (1995) Carotenoid catalism during leaf senescence and its control by light. *J. Photochem. Photobiol. B, Biol.* 30: 3-13.

Bramley, P. M. (2002) Regulation of carotenoid formation during tomato fruit ripening and development. *J. Exp. Bot.* 53: 2107-2113.

Brown, S. B., Houghton, J. D. and Hendry, G. A. F. (1991) Chlorophyll breakdown. *In* Chlorophylls, Edited by Scheer, H., pp. 465-489. CRC Press, Boca Raton, FL.

Chen, B. H. and Chen, Y. Y. (1993) Stability of chlorophylls and carotenoids in sweet potato leaves during microwave cooking. *J. Agric. Food Chem.* 41: 1315-1320.

Chomczynski, P. and Sacchi, N. (1987) Single-step method of RNA isolatopn by acid guanidinium thiocyanate-phenolchloroform extraction. *Anal. Biochem.* 162, 156-159.

Crotty, W. J. and Ledbetter, M. C. (1973) Membrane continuities involving chloroplasts and other organelles in plant cells. *Science* 182: 839-841.

Curty, C., Engel, N. and Gossauer, A. (1995) Evidence for a monooxygenase-catalyzed primary process in the catabolism of chlorophyll. *FEBS Lett.* 364: 41-44.

Doi, M., Shima, S., Egashira, T., Nakamura, K. and Okayama, S. (1997) New bile pigment excreted by a *Chlamydomonas reinhardtii* mutant: A possible breakdown catabolite of chlorophyll *a*. *J. Plant Physiol.* 150: 504-508.

Doi, M., Inage, T. and Shioi, Y. (2001) Chlorophyll degradation in a *Chlamydomonas reinhardtii* mutant: An accumulation of pyropheophorbide *a* by anaerobiosis. *Plant Cell Physiol.* 42: 469-474.

Ekes, M. (1979) Luminal chloroplast connections with endoplasmic reticulum-like cisterns and cell wall in *Dryopteris filix-mas* gametophytes. *Acta biol. Acad. Sci.* Hung. 30: 201-207.

Egger, K. and Schwenker, U. (1966) The esters of lutein in autumn leaves. *Z. Pflanzenphysiol.* 54: 407-416.

Engel, N., Jenny, T. A., Mooser, V. and Gossauer, A. (1991) Chlorophyll catabolism in *Chlorella protothecoides*. Isolation and structure elucidation of a red bilin derivatives. *FEBS Lett*. 293:131-133.

Frohman, M. A., Dush, M. K. and Martin, G. (1988) Rapid production of full-length cDNAs from rare transcripts; amplification using a single gene-specific oligonucleotide primer. *Proc. Natl. Acad. Sci. USA* 85: 8998-9002.

Gossauer, A. and Engel, N. (1996) Chlorophyll catabolism-structures, mechanisms, conversions. *J. Photobiochem. Photobiol. B* 32: 141-151.

Gross, J. (1991) *Pigments in vegetables: chlorophylls and carotenoids.* p. 351. Van Nostrand Reinhold, New York.

Guiamét, J. J., Pichersky, E. and Noodén, L. D. (1999) Mass exodus from senescing soybean chloroplasts. *Plant Cell Physiol.* 40: 986-992.

Guiamét, J. J., Tyystjärvi, E., Tyystjärvi, T., John, I., Kairavuo, M., Pichersky, E. and Noodén, L. D. (2002) Photoinhibition and loss of photosystem II reaction center proteins during senescence of soybean leaves. Enhancement of photoinhibition by the 'stay-green' mutation *cytG*. *Physiol. Plant.* 115: 468-478.

Haidl, H., Knödlmayr, K., Rüdiger, W., Scheer, H., Schoch, S. and Ullrich, J. (1985) Degradation of bacteriochlorophyll *a* in *Rhodopseudomonas sphaeroides* R26. *Z. Naturforsch.* 40c: 685-692.

Hasslacher, M., Schall, M., Hayn, M., Griengl, H., Kohlwein, S. D. and Schwab, H. (1995) Molecular cloning of the full-length cDNA of (S)- hydroxynitrile lyase from *Hevea brasiliensis*: functional expression in *Escherichia coli* and *Saccharomyces serevisiae* and identification of an active residue. *J. Biol. Chem.* 271: 5884-5891.

Higgins, D. G., Thompson, J. D. and Gibson, T. J. (1996) Using CLUSTAL for multiple sequence alignments. *Methods Enzymol.* 266: 383-402.

Hinder, B., Schellenberg, M., Rodoni, S., Ginsburg, S., Vogt, E., Martinoia, E., Matile, P. and Hörtensteiner, S. (1996) How plants dispose of chlorophyll catabolites. *J. Biol. Chem.* 271: 27233-27236.

Hirschberg, J. (2001) Carotenoid biosynthesis in flowering plants. *Curr. Opin. Plant Biol.* 4: 210-218.

Hörtensteiner, S., Vicentini, F and Matile, P. (1995) Chlorophyll breakdown in senescent cotyledons of rape, *Brassica napus* L.: Enzymatic cleavage of pheophorbide *a* in vitro. *New Phytol.* 129: 237-246.

Hörtensteiner, S., Wüthrich, K. L., Matile, P., Ongania, K.-H. and Kräutler, B. (1998) The key step in chlorophyll breakdown in higher plants. Cleavage of pheophorbide *a* macrocycle by a monooxygenase. *J. Biol. Chem.* 273: 15335-15339.

Hörtensteiner, S. (1999) Chlorophyll breakdown in higher plants and algae. *Cell. Mol. Life Sci.* 56: 330-347.

Hyninnen P. H. (1973) Chlorophylls IV. Preparation and purification of some derivatives of chlorophylls *a* and *b*. *Acta Chem. Scand.* 27: 1771-1780.

Ito, H., Tanaka, Y., Tsuji, H. and Tanaka, A. (1993) Conversion of chlorophyll *b* to chlorophyll *a* by isolated cucumber etioplasts. *Arch. Biochem. Biophys.* 306: 148-151.

Iriyama, K., Ogura, N. and Takamiya, A. (1974) A simple method for extraction and partial purification of chlorophyll from plant material, using dioxane. *J. Biochem*. 76: 901-904.

Iturraspe, J. and Moyano, N. (1995) A new 5-formylbilinone as the major chlorophyll *a* catabolite in tree senescent leaves. *J. Org. Chem.* 60: 6664-6665.

Jacob-Wilk, D., Holland, D., Goldschmidt, E. E., Riov, J. and Eyal, Y. (1999) Chlorophyll breakdown by chlorophyllase: isolation and functional expression of the *Chlase1* gene from ethylene-treated *Citrus* fruit and its regulation during development. *Plant J.* 20: 653-661.

Jaskólski, M. (2001) 3D Domain swapping, protein oligomerization, and amyloid formation. *Acta Biochim. Pol.* 48: 807-827.

Jen, J. J. and Mackinney, G. (1970) On the photodecomposition of chlorophyll in vitro-II. Intermediate and breakdown products. *Photochem. Photobiol.* 11: 303-308.

Kato, M. and Shimizu, S. (1985) Chlorophyll metabolism in higher plants VI. Involvement of peroxidase in chlorophyll degradation. *Plant Cell Physiol.* 26: 1291-1301.

Kräutler, B., Jaun, B., Bortlik, K., Schellenberg, M. and Matile, P. (1991) On the enigma of chlorophyll degradation: The constitution of a secoporphinoid catabolite. *Angew. Chem. Intl. Ed.* 30: 1315-1318.

Kurata, H., Maeda, Y., Adachi, M. and Shimokawa, K. (1998) A possible participation of pyropheophorbide *a* in chlorophyll catabolism during ripening of *Citrus unshiu* fruits. *J. Japan Soc. Hort. Sci.* 67: 651-654.

Laemmli U. K. (1970) Cleavage of structural proteins during the assembly of the head of bacteriophage T4. *Nature* 15: 680-685.

Langmeier, M., Ginsburg, S. and Matile, P. (1993) Chlorophyll breakdown in senescent leaves: demonstration of magnesium-dechelatase activity. *Physiol. Plant.* 89: 347-353.

Lightner, D. A. (1977) The photoreactivity of bilirubin and related pyrroles. *Photochem. Photobiol.* 26: 427-436.

Llewellyn, C. A., Mantoura, R. F. C. and Brereton, R. G. (1990a) Products of chlorophyll photodegradation-1. Detection and separation. *Photochem. Photobiol.* 52: 1037-1041.

Llewellyn, C. A., Mantoura, R. F. C. and Brereton, R. G. (1990b) Products of chlorophyll photodegradation-2. Structural identification. *Photochem. Photobiol.* 52: 1043-1047.

Mach, J. M., Castillo, A. R., Hoogstraten, R. and Greenberg, J. T. (2001) The *Arabidopsis*-accelerated cell death gene ACD2 encodes red chlorophyll catabolite reductase and suppresses the spread of disease symptoms. *Proc. Natl. Acad. Sci. USA* 98: 771-776.

Mackinney, G. (1941) Absorption of light by chlorophyll solutions. *J. Biol. Chem.* 140: 315-322.

Matile, P., Hörtensteiner, S., Tomas, H. and Kräutler, B. (1996) Chlorophyll breakdown in senescent leaves. *Plant Physiol.* 122: 1403-1409.

Matile, P., Hörtensteiner, S. and Thomas, H. (1999) Chlorophyll degradation. *Annu. Rev. Plant Physiol. Plant Mol. Biol.* 50: 67-95.

Mühlecker, W., Kräutler, B., Ginsburg, S. and Matile, P. (1993) Breakdown of chlorophyll: the constitution of a secoporphinoid chlorophyll catabolite from senescent rape leaves. *Helv. Chim. Acta* 76: 2976-2980.

Oberhuber, M., Berghold, J., Mühlecker, W., Hörtensteiner, S. and Kräutler, B. (2001) Chlorophyll breakdown – on a nonfluoresent chlorophyll catabolite from spinach. *Helv. Chim. Acta* 84: 2615-2627.

Omata, T. and Murata, N. (1980) A rapid and efficient method to prepare chlorophyll *a* and *b* from leaves. *Photochem. Photobiol.* 31:183-185.

Oshio, Y. and Hase, E. (1969a) Studies on red pigments excreted by cells of *Chlorella protothecoides* during the process of bleaching induced by glucose or acetate I. Chemical properties of the red pigments. *Plant Cell Physiol.* 10: 41-49.

Oshio, Y. and Hase, E. (1969b) Studies on red pigments excreted by cells of *Chlorella protothecoides* during the process of bleaching induced by glucose or acetate II. Mode of formation of the red pigments. *Plant Cell Physiol.* 10: 51-59.

Owens, T. G. and Falkowski, P. G. (1982) Enzymatic degradation of chlorophyll *a* by marine phytoplankton in vitro. *Phytochemistry* 21: 979-984.

Perkins, H. J. and Roberts, D. W. A. (1962) Purification of chlorophylls, pheophytins and pheophorbides for specific activity determinations. *Biochim. Biophys. Acta* 58: 486-498.

Rodoni, S., Mühlecker, W., Anderl, M., Kräutler, B., Moser, D., Thomas, H., Matile, P. and Hörtensteiner, S. (1997) Chlorophyll breakdown in senescent chloroplasts. Cleavage of pheophorbide *a* in two enzymic steps. *Plant Physiol.* 115: 669-676.

Rüdiger, W. (1968) Bile pigments: a new degradation technique and its application. *In* Porphyrins and Related Compounds, Edited by Goodwin, T. W., pp.121-130. Academic Press, London.

Rüdiger, W. (1969) Chromsäure- und Chromatabbau von Gallenfarbstoffen. *Hoppe-Seyler's Z. Physiol. Chem.* 350: 1291-1300.

Schoch, S., Scheer, H., Schiff, J. A., Rüdiger, W. and Siegelman, H. W. (1981) Pyropheophytin *a* accompanies pheophytin *a* in darkened light grown cells of *Euglena*. *Z. Naturforsch.* 36c: 827-833.

Schoch, S. and Vielwerth, F. X. (1983) Chlorophyll degradation in senescent tobacco cell culture (*Nicotiana tabacum* var. "Sumsun"). *Z. Pflanzenphysiol.* 110: 309-317.

Seely, G. R. (1966) The structure and chemistry of functional groups. *In* The Chlorophylls, Edited by Vernon, L. P. and Seely, G. R., pp. 67-109, Academic Press, New York.

Shemin, D. (1957) Biosynthesis of protoporphyrin. *Methods Enzymol.* 4: 643-651.

Shimokawa, K., Hashizume, A. and Shioi, Y. (1990) Pyropheophorbide *a*, a catabolite of ethylene-induced chlorophyll *a* degradation. *Phytochemistry* 29: 2105-2106.

Shimomura, O. (1980) Chlorophyll-derived bile pigment in bioluminescent euphausiids. *FEBS Lett.* 116: 203-206.

Shioi, Y., Tatsumi, Y. and Shimokawa, K. (1991) Enzymatic degradation of chlorophyll in *Chenopodium album*. *Plant Cell Physiol.* 32: 87-93.

Shioi, Y., Watanabe, K., Takamiya, K., Garrido, J. L. and Zapata, M. (1995) Separation of mono- and divinyl chlorophyll species by high-performance liquid chromatography using an octadecyl polyvinyl alcohol polymer column. *Anal. Biochem.* 231: 225-229.

Shioi, Y., Tomita, N., Tsuchiya, T. and Takamiya, K. (1996a) Conversion of chlorophyllide to pheophorbide by Mg-dechelating substance in extracts of *Chenopodium album*. *Plant Physiol. Biochem.* 34: 41-47.

Shioi, Y., Watanabe, K. and Takamiya, K. (1996b) Enzymatic conversion of pheophorbide *a* to the precursor of pyropheophorbide *a* in leaves of *Chenopodium album*. *Plant Cell Physiol.* 37: 1143-1149.

Suzuki, Y., Tanabe, K. and Shioi, Y. (1999) Determination of chemical oxidation products of chlorophyll and porphyrin by high-performance liquid chromatography. *J. Chromatogr. A* 839: 85-91.

Suzuki, Y. and Shioi, Y. (1999) Detection of chlorophyll breakdown products in the senescent leaves of higher plants. *Plant Cell Physiol.* 40: 909-915.

Suzuki, Y. and Shioi, Y. (2001) Degradation of chlorophylls: Two reaction pathways in the formation of pyropheophorbide *a*. *PS2001 Proceedings (12th International Congress of Photosynthesis)*, S2-021. CSIRO Publishing, Collingwood, Vic.

Suzuki, Y., Doi, M. and Shioi, Y. (2002) Two enzymatic reaction pathways in the formation of pyropheophorbide *a*. *Photosynth. Res.* 74: 225-233.

Suzuki, Y. and Shioi, Y. (2003) Identification of chlorophylls and carotenoids in major teas by high performance liquid chromatography with photodiode array detection. *J. Agric. Food Chem.* 51 (in press)

Svec, W. A. (1978) The isolation, preparation, characterization, and estimation of the chlorophylls and the bacteriochlorophylls. *In* The Porphyrins, Edited by Dolphin, D., Vol. 5, pp. 341-399. Academic Press, New York.

Takamiya, K., Tsuchiya, T. and Ohta, H. (2000) Degradation pathway(s) of chlorophyll: what has gene cloning revealed? *Trends Plant Sci.* 5: 426-431.

Tevini, M. and Steinmüller, D. (1985) Composition and function of plastoglobuli II. Lipid composition of leaves and plastoglobuli during beech leaf senescence. *Planta* 163: 91-96.

Tsuchiya, T., Ohta, H., Masuda, T., Mikami, B., Kita, N., Shioi, Y. and Takamiya, K. (1997) Purification and characterization of two isozymes of chlorophyllase from mature leaves of *Chenopodium album*. *Plant Cell Physiol.* 38: 1026-1031.

Tsuchiya, T., Ohta, H., Okawa, K., Iwamatsu, A., Shimada, H., Masuda, T. and Takamiya, K. (1999) Cloning of chlorophyllase, the key enzyme in chlorophyll degradation: Finding of a lipase motif and the induction by methyl jasmonate. *Proc. Natl. Acad. Sci. USA* 96: 15362-15367.

Tsuchiya, T., Suzuki, T., Yamada, T., Shimada, H., Masuda, T., Ohta, H., and Takamiya, K. (2003) Chlorophyllase as a serine hydrolase: Identification of a putative catalytic triad. *Plant Cell Physiol.* 44: 96-101.

Vaughn, K. C. and Duke, S. O. (1981) Evaginations from the plastid envelope: a method for transfer of substances from plastid to vacuole. *Cytobios* 32: 89-95.

Vicentini, F., Iten, F. and Matile, P. (1995) Development of an assay for Mg-dechelatase of oilseed rape cotyledons, using chlorophyllin as the substrate. *Physiol. Plant*. 94: 57-63.

Walmsley, J and Adamson, H. (1994) Chlorophyll turnover in etiolated greening barley transferred to darkness: Isotopic (1-^{14}C glutamic acid) evidence of dark chlorophyll synthesis in the absence of chlorophyll accumulation. *Physiol. Plant.* 94: 57-63.

Watanabe, K., Tsuchiya, T., Masuda, T., Ohta, H., Takamiya, K. and Shioi, Y. (1995) Characterization and some properties of pheophorbidase from *Chenopodium album. In* Photosynthesis: from Light to Biosphere, Edited by Mathis, P., Vol. 3, pp. 981-984. Kluwer Academic Publishers, Dordrecht.

Watanabe, K., Ohta, H., Tsuchiya, T., Mikami, B., Masuda, T., Shioi, Y. and Takamiya, K. (1999) Purification and some properties of pheophorbidase in *Chenopodium album*. *Plant Cell Physiol*. 40: 104-108.

Wellburn, F. A. M. and Wellburn, A. R. (1979) Conjoined mitochondria and plastids in the barley mutant *albostrians*. *Planta* 147: 178-179.

Whitfield, D. M. and Roean, K. S. (1974) Changes in the chlorophylls and carotenoids of leaves of *Nicotina tabacum* during senescence. *Phytochemistry* 13: 77-83.

Willstätter, R and Stoll, A (1913) Die Wirkungen der Chlorophyllase. *In* Untersuchungen über Chlorophyll. pp. 172-187. Springer, Berlin.

Wüthrich, K. L., Bovet, L., Hunziker, P. E., Donnison, I. S. and Hörtensteiner, S. (2000) Molecular cloning, functional expression and characterization of RCC reductase involved in chlorophyll catabolism. *Plant J.* 21: 189-198.

Zapata, M., Rodríguez, F. and Garrido, J. L. (2000) Separation of chlorophylls and carotenoids from marine phytoplankton: A new HPLC method using a reversed phase C_8 column and pyridine-containing mobile phases. *Mar. Ecol. Prog. Ser.* 195: 29-45.

Ziegler, R., Blaheta, A., Guha, N. and Schönegge, B. (1988) Enzymatic formation of pheophorbide and pyropheophorbide during chlorophyll degradation in a mutant of *Chlorella fusca* Shihira et Kraus. *J. Plant Physiol.* 132: 327-332.

Acknowledgements

I wish to express my sincere gratitude to Dr. Yuzo Shioi, Professor of Shizuoka University, for his supervision, generous advice and encouragement during this work. I greatly appreciate to Dr. Toyoki Amano, Shizuoka University, for his helpful advice and suggestion.

I thank all members of Shioi's laboratory for fully cooperation in my research.

List of Publications

Suzuki, Y., Tanabe, K. and Shioi, Y. (1999) Determination of chemical oxidation products of chlorophyll and porphyrin by high-performance liquid chromatography. Journal of Chromatography A839: 85-91.

Suzuki, Y. and Shioi, Y. (1999) Detection of chlorophyll breakdown products in the senescent leaves of higher plants. Plant and Cell Physiology 40: 909-915.

Suzuki, Y., Doi, M. and Shioi, Y. (2002) Degradation of chlorophylls: Two reaction pathways in the formation of pyropheophorbide *a*. Photosynthesis Research 72: 225-233.

Suzuki, Y. and Shioi, Y. (2003) Identification of chlorophylls and carotenoids in major teas by high-performance liquid chromatography with photodiode array detection. Journal of Agricultural and Food Chemistry 51 (in press)